ELSEVIER

Colloids and Surfaces
A: Physicochemical and Engineering Aspects 96 (1995) 1–46

COLLOIDS AND SURFACES A

Review

Poly(ethylene oxide)–poly(propylene oxide)–poly(ethylene oxide) block copolymer surfactants in aqueous solutions and at interfaces: thermodynamics, structure, dynamics, and modeling

Paschalis Alexandridis, T. Alan Hatton*

Department of Chemical Engineering, Massachusetts Institute of Technology, 77 Massachusetts Avenue, Cambridge, MA 02139, USA

Received 18 July 1994; accepted 17 September 1994

Abstract

The association properties of poly(ethylene oxide)-*block*-poly(propylene oxide)-*block*-poly(ethylene oxide) (PEO-PPO-PEO) copolymers (commercially available as Poloxamers and Pluronics) in aqueous solutions, and the adsorption of these copolymers at interfaces are reviewed. At low temperatures and/or concentrations the PEO-PPO-PEO copolymers exist in solution as individual coils (unimers). Thermodynamically stable micelles are formed with increasing copolymer concentration and/or solution temperature, as revealed by surface tension, light scattering, and dye solubilization experiments. The unimer-to-micelle transition is not sharp, but spans a concentration decade or 10 K. The critical micellization concentration (CMC) and temperature (CMT) decrease with an increase in the copolymer PPO content or molecular weight. The dependence of CMC on temperature, together with differential scanning calorimetry experiments, indicates that the micellization process of PEO–PPO–PEO copolymers in water is endothermic and driven by a decrease in the polarity of ethylene oxide (EO) and propylene oxide (PO) segments as the temperature increases, and by the entropy gain in water when unimers aggregate to form micelles (hydrophobic effect). The free energy and enthalpy of micellization can be correlated to the total number of EO and PO segments in the copolymer and its molecular weight. The micelles have hydrodynamic radii of approximately 10 nm and aggregation numbers in the order of 50. The aggregation number is thought to be independent of the copolymer concentration and to increase with temperature. Phenomenological and mean-field lattice models for the formation of micelles can describe qualitatively the trends observed experimentally. In addition, the lattice models can provide information on the distribution of the EO and PO segments in the micelle. The PEO–PPO–PEO copolymers adsorb on both air–water and solid–water interfaces; the PPO block is located at the interface while the PEO block extends into the solution, when copolymers are adsorbed at hydrophobic interfaces. Gels are formed by certain PEO–PPO–PEO block copolymers at high concentrations, with the micelles remaining apparently intact in the form of a "crystal". The gelation onset temperature and the thermal stability range of the gel increase with increasing PEO block length. A comparison of PEO–PPO copolymers with PEO–PBO and PEO–PS block copolymers and C_iE_j surfactants is made, and selected applications of PEO–PPO–PEO block copolymer solutions (such as solubilization of organics, protection of microorganisms, and biomedical uses of micelles and gels) are presented.

Keywords: Block copolymer surfactants; Dynamics; Interfaces; Modeling; Structure; Thermodynamics

* Corresponding author.

SSDI 0927-7757(94)03028-6

1. Introduction

Copolymers are synthesized by the simultaneous polymerization of more than one type of monomer. The result of such a synthesis is called a block copolymer if the individual monomers occur as blocks of various lengths in the copolymer molecule. The different types of blocks within the copolymer are usually incompatible with one another and, as a consequence, block copolymers self assemble in melts and in solutions. In the case of amphiphilic copolymers in aqueous solutions, the copolymers can assemble in microstructures that resemble micelles formed by low-molecular-weight surfactants.

Water-soluble triblock copolymers of poly(ethylene oxide) (PEO) and poly(propylene oxide) (PPO), often denoted PEO–PPO–PEO or $(EO)_{n1}(PO)_m(EO)_{n2}$, are commercially available nonionic macromolecular surface active agents. Variation of the copolymer composition (PPO/PEO ratio) and molecular weight (PEO and PPO block length) during synthesis leads to the production of molecules with optimum properties that meet the specific requirements in various areas of technological significance. As a result, PEO–PPO–PEO block copolymers are an important class of surfactants and find widespread industrial applications in [1,2] detergency, dispersion stabilization, foaming, emulsification, lubrication, and formulation of cosmetics [3,4] and inks [5,6], etc., along with more specialized applications in, for example, pharmaceuticals (drug solubilization and controlled release [7–10] and burn wound covering [11]), bioprocessing (protecting microorganisms against mechanical damage [12–14]), and separations (solubilization of organics in aqueous solutions [15–17]). Commercial names for these surfactants are Poloxamers (manufactured by ICI) and Pluronics (manufactured by BASF).

2. Synthesis, nomenclature, and physical properties

The PEO–PPO–PEO triblock copolymers are synthesized by the sequential addition of first propylene oxide (PO) and then ethylene oxide (EO) to a low molecular weight water-soluble propylene glycol, a poly(propylene oxide) oligomer (note that propylene glycol changes from water soluble to water insoluble as the molecular weight increases beyond about 740). The oxyalkylation steps are carried out in the presence of an alkaline catalyst, generally sodium or potassium hydroxide. The catalyst is then neutralized and removed from the final product [1]. The equations representing the two steps in the synthesis of the PEO–PPO–PEO copolymers are shown in Fig. 1.

The Pluronic PEO–PPO–PEO block copolymers are available in a range of molecular weights and PPO/PEO composition ratios [1,2,18]. The Pluronic copolymers are presented in Fig. 2, arranged in the so-called "Pluronic grid" [2,18]. The copolymers along the vertical lines have the same PPO/PEO composition, while the copolymers along the horizontal lines have PPO blocks of the same length. The notation for the Pluronic triblock copolymers starts with the letters L (for liquid), P (for paste), or F (for flakes). The first one or two numbers are indicative of the molecular weight of the PPO block, and the last number signifies the weight fraction of the PEO block. For example, Pluronics P104 and F108 have the same molecular weight of PPO (in the order of 3000), but P104 has 40 wt.% PEO and F108 80 wt.% PEO. The notation of Fig. 2 will be used in the ensuing discussion.

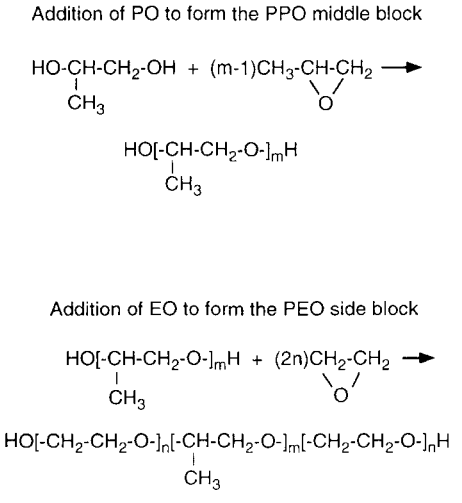

Fig. 1. Equations representing the synthesis of the PEO–PPO–PEO copolymers.

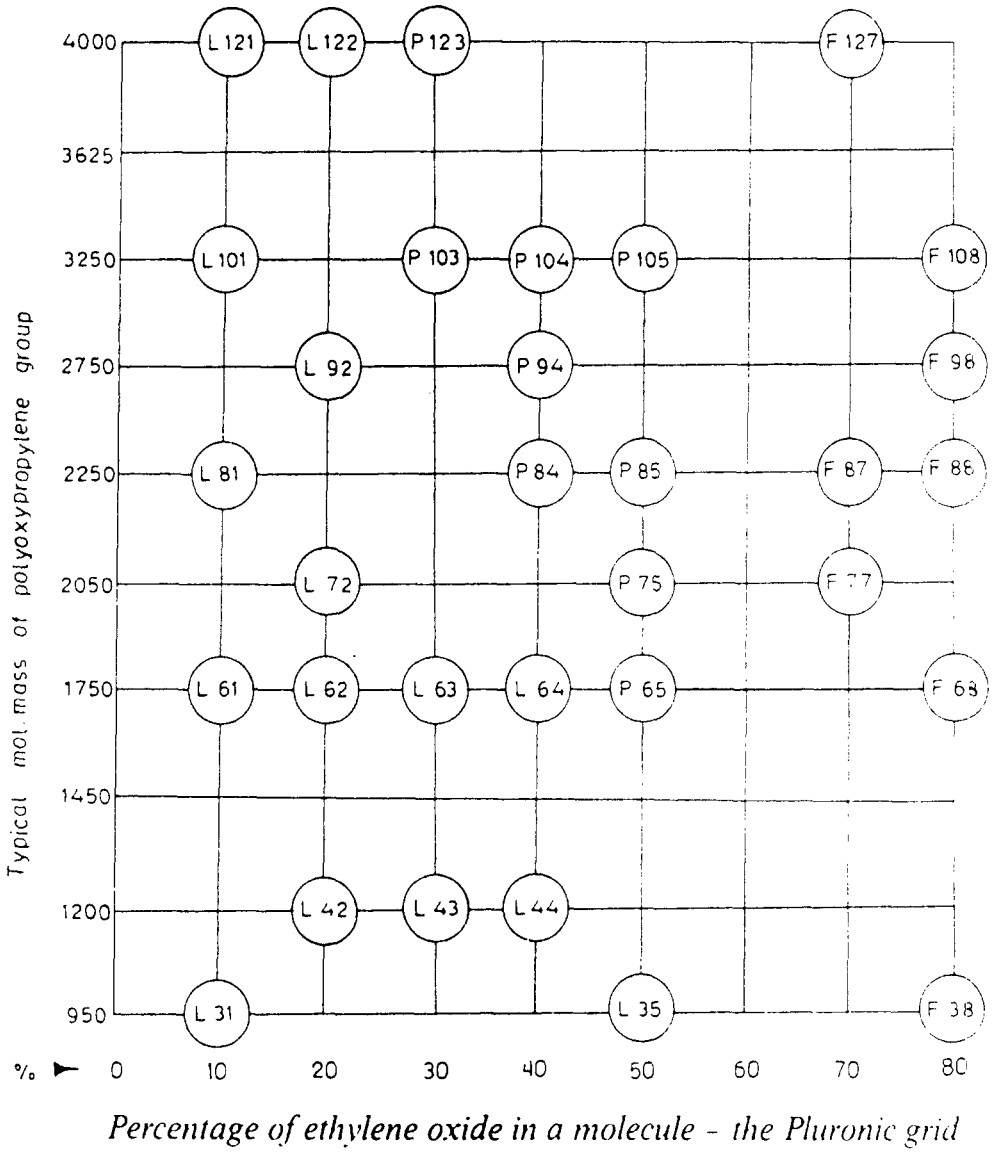

Fig. 2. Pluronic PEO–PPO–PEO copolymers arranged in the "Pluronic grid". The copolymers along the vertical lines have the same PPO/PEO composition ratio, while the copolymers along the horizontal lines have PPO blocks of the same length. (Reprinted with permission from Ref. [2]; copyright Carl Hanser Verlag, 1991.)

Some of the physical properties (average molecular weight, melting/pour point, viscosity, surface tension, foam height, cloud point and hydrophilic–lipophilic balance) of the Pluronic PEO–PPO–PEO copolymers are listed in Table 1 (data supplied by the manufacturer [18]). The cloud point, the temperature at which the copolymers phase separate from water, ranges from approximately 10 C for copolymers with low PEO content to above 100°C for copolymers with high PEO content. The PEO content also influences the rate of dissolution: this rate decreases as the relative proportion of the PEO block increases. The dissolution rate also decreases as the copolymer molecular weight increases for Pluronic copolymer groups with the same PPO/PEO com-

Table 1
Properties of the Pluronic PEO–PPO–PEO copolymers

A	B	C	D	E	F	G	H	I
L35	1900	50	7	375	49	25	73	18–23
F38	4700	80	48	260	52	35	>100	>24
L42	1630	20	−26	280	46	0	37	7–12
L43	1850	30	−1	310	47	0	42	7–12
L44	2200	40	16	440	45	25	65	12–18
L62	2500	20	−4	450	43	25	32	1–7
L63	2650	30	10	490	43	30	34	7–12
L64	2900	40	16	850	43	40	58	12–18
P65	3400	50	27	180	46	70	82	12–18
F68	8400	80	52	1000	50	35	>100	>24
L72	2750	20	−7	510	39	15	25	1–7
P75	4150	50	27	250	43	100	82	12–18
F77	6600	70	48	480	47	100	>100	>24
P84	4200	40	34	280	42	90	74	12–18
P85	4600	50	34	310	42	70	85	12–18
F87	7700	70	49	700	44	80	>100	>24
F88	11400	80	54	2300	48	80	>100	>24
F98	13000	80	58	2700	43	40	>100	>24
P103	4950	30	30	285	34	40	86	7–12
P104	5900	40	32	390	33	50	81	12–18
P105	6500	50	35	750	39	40	91	12–18
F108	14600	80	57	2800	41	40	>100	>24
L122	5000	20	20	1750	33	20	19	1–7
P123	5750	30	31	350	34	45	90	7–12
F127	12600	70	56	3100	41	40	>100	18–23

A: copolymer. B: average molecular weight. C: PEO wt.%. D: melting pour point (°C). E: viscosity (Brookfield) (cps; liquids at 25°C, pastes at 60°C, solids at 77°C). F: surface tension at 0.1%, 25°C (dyn cm^{-1}). G: foam height (mm) (Ross Miles, 0.1% at 50°C). H: cloud point in aqueous 1% solution (°C). I: HLB (hydrophilic–lipophilic balance).

position ratio [1]. This is probably a result of the degree of hydrogen bonding between the copolymer molecules, and is also reflected in the physical form of the copolymers (liquid for low molecular weight, low PEO content; solid for high molecular weight, high PEO content copolymers). The PEO–PPO–PEO copolymers exhibit maximum foam height at a PPO/PEO ratio of 40:60; foam properties of each copolymer series increase and then decrease slightly as the molecular weight of the PPO segment increases; copolymers with high PPO content are effective defoamers [1]. Attempts to correlate the emulsification properties with PPO/PEO ratio and PPO molecular weight have not been very successful; copolymers with PPO blocks of high molecular weight are generally better emulsifiers than the lower-molecular-weight homologs [1]. The thickening power of each series of copolymers increases as the PPO block molecular weight increases and as the PPO/PEO ratio decreases.

3. Micelle formation in PEO–PPO–PEO block copolymer aqueous solutions

3.1. Techniques for detecting CMC and CMT

The critical micellization concentration (CMC), the amphiphile concentration at which micelles (thermodynamically stable polymolecular aggregates) start forming, is a parameter of great fundamental value [19,20]. The micellization of amphiphilic block copolymers is inherently more complex than that of conventional, low-molecular-weight surfactants. The composition polydispersity could be appreciable even for a copolymer with a narrow molecular weight distribution and, accordingly, no sharp CMC or CMT (critical micellization temperature, the copolymer solution temperature at which micelles form) have been observed for block copolymers. In practice, a certain CMC range with some notable uncertainty is usually detected. A large difference is often noted between the CMC values determined by different methods because the sensitivity of the techniques to the quantity of molecularly dispersed copolymers (unimers) present in solution may vary [21]. For common surfactants, a considerable amount of CMC data has been collected and summarized by Mukerjee and Mysels [22], whereas for block copolymers only scarce CMC data have been available in the literature so far (see, for example, Refs. [23] and [24]). Further, the values reported in the literature differ substantially; the lack of sufficient temperature control, in conjunction with batch-to-batch variations, may be responsible for the observed variations [25].

Light scattering and fluorescence spectroscopy experiments have shown that PEO–PPO–PEO block copolymers of suitable PPO/PEO composition and molecular weight do indeed form polymolecular aggregates in solution. As discussed below, the CMC of aqueous PEO–PPO–PEO copolymer

solutions decreases with increasing temperature [21,26–28]. Micellar growth was observed for Pluronic L64 with an increase in the copolymer concentration at 25°C [29]; micelle formation by Pluronic P85 was investigated by Brown et al. [27] using static and dynamic light scattering. It was found that unimers, micelles, and "micellar aggregates" coexisted; the relative proportions of each species depended strongly on temperature and copolymer concentration. Micellar growth occurred with increasing temperature as evidenced when the scattering intensity of a 4.8% P85 solution was recorded as a function of temperature; a sharp increase in the scattering intensity at approximately 30°C denoted the formation of micelles. A significant temperature dependence was also observed in the micellization behavior of Pluronic F68 [21]. Using static and dynamic light scattering, Zhou and Chu [21] detected three temperature regions, which they called the unimer, transition, and micelle regions, respectively. At room temperature, "particles" with a hydrodynamic radius of around 2.3 nm and a broad polydispersity were detected. Above 50 C, micelle molecular weights were found to increase linearly with temperature, while the hydrodynamic radius remained constant, at approximately 8 nm [21]. Wanka et al. [30] confirmed the finding of Zhou and Chu, that aggregation numbers increase with temperature, while the micelle radius remains approximately constant. More information on Pluronic copolymer micelle size and aggregation numbers, determined by scattering techniques, is presented in Section 5.1.

Spectroscopic techniques, based either on optical absorption or on emission of light from some "probe" molecule, are now well established for investigating a wide range of physical properties of micellar solutions [19,31]. Fluorescence probes were employed by Turro and Chung [32] in studying the behavior of a poly(ethylene oxide)–poly(propylene oxide) block copolymer in water. The polymer they used had a total molecular weight of 3000, with a PEO/PPO molar ratio of 0.8; it was not specified in the paper whether it was a di- or triblock copolymer. Regions of no aggregation, "monomolecular" micelles (attributed to a change in the copolymer segment conformation to a more compact structure), and polymolecular micelles were identified with increasing polymer concentration. The aggregation number of the micelles formed at high polymer concentration was determined to be 52. With an increase in temperature, a hydrophobic fluorescence probe (expected to reside in the micelle core) experienced a more hydrophilic environment, whereas a hydrophilic probe (expected to reside in the interfacial region) experienced a more hydrophobic environment. This observation was attributed to a greater mixing of PEO chains in the hydrophobic micelle core at higher temperatures owing to increased thermal agitation.

A hydrophobic fluorescence probe (diphenylhexatriene, DPH) was used by Alexandridis et al. [28] to determine the onset of micellization for a number of Pluronic block copolymers in aqueous solutions. The fluorescence efficiency of DPH is zero in a hydrophilic environment and unity in a hydrophobic environment (such as the core of a micelle), thus providing a sensitive indicator of micelle formation with increasing solution temperature and copolymer concentration. CMC and CMT data were obtained and correlated to the Pluronic molecular weight and PPO/PEO ratio [28]. Fig. 3 shows the intensity of absorbed light (arbitrary units) due to DPH as a function of temperature for aqueous Pluronic P104 solutions

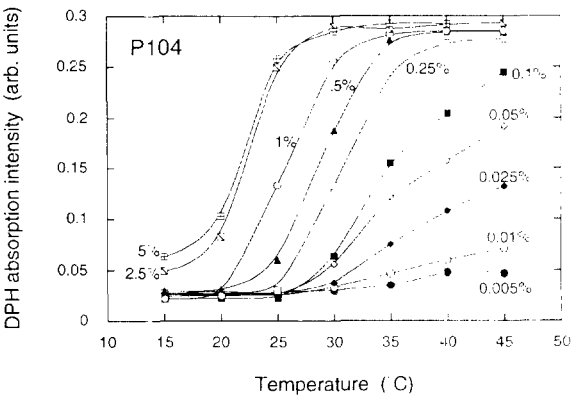

Fig. 3. Light absorption (arbitrary units) due to DPH as a function of temperature for aqueous Pluronic P104 solutions at various copolymer concentrations; the critical micellization temperature values were obtained from the first break in the sigmoidal curves. (Adapted with permission from Ref. [28]; copyright American Chemical Society, 1994.)

at various copolymer concentrations [28]; the critical micelle temperature values were obtained from the first break in the intensity vs. temperature sigmoidal curves. Critical micelle concentrations can be obtained in a similar manner from intensity vs. log(concentration) plots. Chattopadhyay and London [33] used the fluorescence emission of DPH to determine the CMC of various surfactants, and obtained values that were within 10% of those determined by other techniques. Surface tension results showed that probe molecules, at the levels used to determine the CMC by fluorescence (probe concentration $<10^{-6}$ kmol m^{-3}), did not noticeably affect the surfactant properties, notably surface tension, nor the surface tension-derived CMC value [34]. Edwards et al. [35] reported that, in general, the CMC values they obtained from the surface tension data for solutions of deionized water and non-ionic surfactants showed fairly close agreement with the CMC values inferred from polyaromatic hydrocarbon solubilization data. Similar values for the CMC of the PEO–PPO–PEO block copolymers measured by surface tension and dye solubilization methods have been reported by Schmolka and Raymond [36]. The use of surface tension measurements for the determination of CMC in PEO–PPO–PEO copolymer solutions is discussed in detail in Section 7.1.

Alexandridis et al. [37] reported the effects of temperature on the micellization properties and the structure of the micelles for Pluronics P104 and F108, PEO–PPO–PEO block copolymers having similar size hydrophobic (PPO) block and different size hydrophilic (PEO) blocks. CMC and CMT data for aqueous copolymer solutions were obtained from a dye solubilization method [28] and corroborated with differential scanning calorimetry (DSC), surface tension, density, light scattering intensity, and fluorescence spectroscopy experiments. Best agreement between the different techniques was achieved when the critical micellization data were estimated from (i) the onset of solubilization of a hydrophobic dye, (ii) the onset of the endothermic transition observed in DSC, (iii) the high-concentration break in the surface tension vs. polymer concentration curve, (iv) the first break in the partial specific volume vs. temperature curve, (v) the onset of increased light scattering intensity, and (vi) the inflexion in the pyrene fluorescence emission intensity I_1/I_3 ratio (see Section 5.2.) vs. temperature sigmoidal curve [37]. These guidelines should facilitate the reporting of consistent CMC and CMT data for amphiphilic copolymer solutions.

3.2. Effect of copolymer composition and molecular weight on micelle formation

It is apparent from the experimental studies that PEO–PPO–PEO copolymers which are relatively less hydrophobic, either due to a high PEO content or a low molecular weight, do not form micelles at room temperature, but do start to aggregate at higher temperatures. This can be explained by the fact that water becomes a poorer solvent for both ethylene oxide and propylene oxide segments at higher temperatures. As shown by Alexandridis et al. [28], the micellization process is strongly driven by entropy, and the free energy of micellization is mainly a function of the PPO block, the hydrophobic part of the copolymer.

For groups of PEO–PPO–PEO copolymers with PEO blocks of constant molecular weight and PPO blocks of varying molecular weight, the CMC values for the Pluronic solutions (at a given solution temperature) decreased with increasing number of PO segments, indicating that polymers with a larger hydrophobic (PPO) domain form micelles at lower concentrations [28]. Higher temperatures resulted in lower CMC values, with the slope of the log(CMC) vs. PO-segment-number curve increasing with temperature. The CMT values for the Pluronic copolymer solutions (at a given copolymer concentration) also decreased as a function of the number of PO segments, indicating that polymers with a larger hydrophobic domain form micelles at lower temperatures. The CMC and CMT values for groups of Pluronic copolymers with hydrophobic blocks of constant length and hydrophilic blocks of varying length, e.g. with 30 (L64, P65, F68), 40 (P84, P85, F88), and 60 (P104, P104, F108) PO segments, showed a small increase in the CMC and CMT with increasing number of EO segments. This would indicate that micelle formation becomes more difficult the more hydrophilic the molecules,

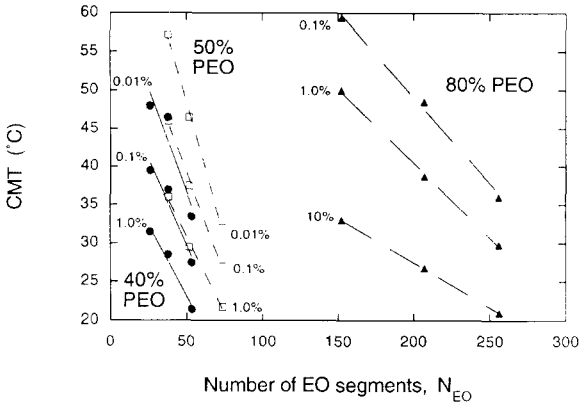

Fig. 4. Critical micellization temperatures at various PEO–PPO–PEO copolymer concentrations, as a function of the number of EO segments, for copolymers with 40, 50, and 80% PEO content. (Reprinted with permission from Ref. [28]; copyright American Chemical Society, 1994.)

although the effect of PEO on the CMC and CMT is less pronounced than that of PPO, intimating that PPO is a primary factor in the micellization process. The CMC and CMT values for copolymers of constant PPO/PEO composition ratio decreased with increasing molecular weight. The CMT values were influenced more by molecular weight the lower the relative PEO content and the lower the copolymer concentration, as is evidenced by the steeper slopes for the curves for these conditions. These trends are shown in Fig. 4 [28].

4. Micellization thermodynamics

4.1. Association model, differential scanning calorimetry

It is well established that block copolymers of the A–B or A–B–A type form micelles in selective solvents which are thermodynamically good solvents for one block and precipitants for the other. In general, micellization of block copolymers, as in the case of conventional surfactants, obeys the closed association model, which assumes an equilibrium between molecularly dispersed copolymer (unimer) and multimolecular aggregates (micelles) [24,38]. There are two main approaches to the thermodynamic analysis of the micellization process: the phase separation model, in which the micelles are considered to form a separate phase at the CMC, and the mass-action model that considers micelles and unassociated unimers to be in an association–dissociation equilibrium [39]. In both approaches, the standard free energy change for the transfer of 1 mol of amphiphile from solution to the micellar phase, ΔG° (the free energy of micellization), in the absence of electrostatic interactions (the PEO–PPO–PEO copolymers are non-ionic) is given by [19,39]

$$\Delta G^{\circ} = RT \ln(X_{CMC}) \quad (1)$$

where R is the gas law constant, T is the absolute temperature, and X_{CMC} is the critical micellization concentration in mole fraction units. In order to obtain this simple expression, the assumption has been made that the concentration of free surfactant (unimer) in the presence of micelles is constant and equal to the CMC value, in the case of the phase-separation model, or that the micelle aggregation number is large for the mass-action model. Applying the Gibbs–Helmholtz equation, we can express the standard enthalpy of micellization, ΔH°, as [19,39]

$$\Delta H^{\circ} = -RT^2[\partial \ln(X_{CMC})/\partial T]_P$$
$$= R[\partial \ln(X_{CMC})/\partial(1/T)]_P \quad (2)$$

Finally, the standard entropy of micellization per mole of surfactant, ΔS°, can be obtained from

$$\Delta S^{\circ} = (\Delta H^{\circ} - \Delta G^{\circ})/T \quad (3)$$

It has been shown for block copolymer micellization [40] that, within experimental error,

$$\partial \ln(X_{CMC})/\partial(1/T) = \partial \ln(X)/\partial(1/T_{CMT}) \quad (4)$$

where X is the concentration expressed as a mole fraction, and T_{CMT} is the critical micellization temperature; thus Eq. (2) becomes

$$\Delta H^{\circ} = R[\partial \ln(X)/\partial(1/T_{CMT})]_P \quad (5)$$

In accordance with Eq. (5), the inverse T_{CMT} values are shown as a function of the logarithm of copolymer concentration (mole fraction units) for a number of Pluronic copolymers in Fig. 5 [28]. The T_{CMT} data, plotted in this manner, generally showed linearity. The use of the closed association

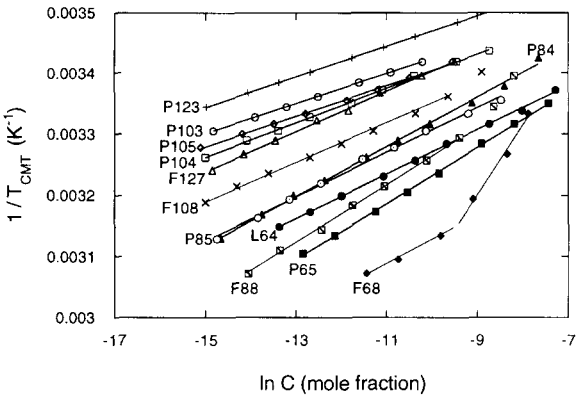

Fig. 5. Reciprocal T_{CMT} vs. copolymer concentration plots for various Pluronic PEO–PPO–PEO copolymers; the plots were used for determination of the micellization enthalpy in terms of the closed association model. (Reprinted with permission from Ref. [28]; copyright American Chemical Society, 1994.)

model appeared well justified based on the good fit; such a model was consequently employed for estimating ΔH° and ΔS° of the micellization process [28]. Note that the major assumption involved in deriving Eqs. (1)–(5) is based on the micelle aggregation number (N) being sufficiently large that the terms $RTN^{-1}\ln N$ and $RTN^{-1}\ln X_{mic}$ (where X_{mic} is the mole fraction of micelles) can be omitted from the right-hand-side of Eq. (1) [19]. For a typical aggregation number of 50, $N^{-1}\ln N \approx 0.08$, indeed negligible compared to the value of $|\ln X_{CMC}|$ (in the range 10–15). Using the same aggregation number and concentrations $X_{CMC} = 6 \times 10^{-6}$ and $X_{mic} = 6 \times 10^{-10}$, the magnitude of the $|N^{-1}\ln X_{mic}|$ term is 0.4, approximately 3% of the $|\ln X_{CMC}|$ (≈ 12) term; the temperature derivatives of the $RTN^{-1}\ln N$ and $RTN^{-1}\ln X_{mic}$ terms that should appear in Eq. (2) are also negligible.

The standard enthalpy of micellization, ΔH°, was calculated from the inverse slope of the linear fit to the $1/T_{CMT}$ vs. ln(mole fraction) data, in accordance with Eq. (5). ΔH° values, together with ΔG° and ΔS° (calculated from Eqs. (1) and (3), respectively, at the critical micellization temperature for 1% copolymer solutions), are listed in Ref. [28] for various Pluronic PEO–PPO–PEO copolymers. The tabulated values of ΔH°, ΔG°, and ΔS° ranged from 169 to 339 kJ mol^{-1}, -24.5 to -28.8 kJ mol^{-1}, and 0.638 to 1.244 kJ mol^{-1} K^{-1}, respectively. The higher values of ΔH°, ΔG°, and ΔS° were observed for Pluronics P103 and L64, while the lower values were observed for the relatively hydrophilic Pluronic copolymers F68 and F88. The standard enthalpy of micellization, ΔH°, is positive, indicating that the transfer of unimers from solution to the micelle is an enthalpically unfavorable endothermic process. The free energy, ΔG°, is negative, since thermodynamically stable micelles are formed spontaneously. Thus, it becomes clear that a negative entropy contribution must be the driving force for micellization of the block copolymers; note that, in contrast to the entropy-driven micellization in water, the micellization of copolymers in non-polar solvents originates from enthalpy interactions between the copolymer segments and the solvent [24]. The traditional view of micelle formation [19,41] is based on the "hydrophobic effect" [42,43]. The presence of hydrocarbon molecules in water causes a significant decrease in the entropy of the latter, suggesting an increase in the degree of structuring of the water molecules. When hydrocarbon residues aggregate in aqueous solution to form a micelle, the hydrogen bonding structure in the water is restored and the water entropy increases, overcoming the entropy loss due to the localization of the hydrophobic chains in the micelles. The entropy contribution usually dominates the micellization process in aqueous surfactant solutions, with the enthalpy playing a minor role [19]. The magnitude of the hydrophobic effect increases with temperature [43], in agreement with the observed increased tendency for micelle formation with increasing temperature; however, such an explanation does not take into account the specific nature of the PEO–PPO–PEO copolymers.

Solute–solvent [44,45] or solute–solute interactions [46] have also been proposed in order to interpret the "molecular-level" mechanism behind the temperature dependence observed in the micellization of PEO–PPO–PEO copolymers in water (note that the hydrophobic effect outlined above is based on solvent–solvent interactions). Kjelander and Florin [44] attempted to reproduce the negative entropy and enthalpy of water–PEO mixing and the phase diagram of the PEO–water system,

assuming a zone with increased structuring of water to exist around the PEO chain. The phase separation that takes place at high temperatures was attributed to a breakdown of the zones of enhanced water structure. Kjelander and Florin [44] claim that when PPO is introduced into water it also develops a hydration shell with an enhanced water structure, but since the methyl groups of PPO provide steric hindrance, the water structure is weak and leads to phase separation. Karlstrom [46] predicted the PEO–water phase diagram using Flory–Huggins theory and assuming that each segment of the PEO chain can exist in two forms, one polar with a low energy and a low statistical weight, and one less polar, or non-polar, with a higher energy and statistical weight. The polar conformations dominate at low temperatures making the solute–solvent interaction favorable, whereas at higher temperatures the non-polar class of states becomes increasingly populated, rendering the solute–solvent interaction less favorable [47]. The model for predicting the solution behavior of block copolymer micelles developed by Hurter et al. [48,49] and Linse [50,51] (see Section 6.2. for a description of this model) incorporated Karlstrom's ideas to account for the conformational distribution in PEO and PPO; the model predictions agree with the trends observed experimentally, thus supporting the polar–non-polar state model as an explanation of the effect of temperature on the solution behavior of PEO and PPO.

Another method for obtaining estimates of the enthalpy of micellization, ΔH°, is DSC. DSC measurements for aqueous Pluronic copolymer solutions show endothermic peaks [30,52], typical for a first-order phase transition, at concentration-dependent characteristic temperatures as shown in Fig. 6 [37]. The peaks yield rather high enthalpy values and are broad, extending more than 10 K. The latter observation has been attributed to the fact that the copolymers are not pure compounds but show a broad molar weight distribution; it is known that melting peaks become broad in the presence of impurities [30]. It should be pointed out that the enthalpy change measured by the peak area in DSC is not the standard enthalpy change, but depends upon the real states of the

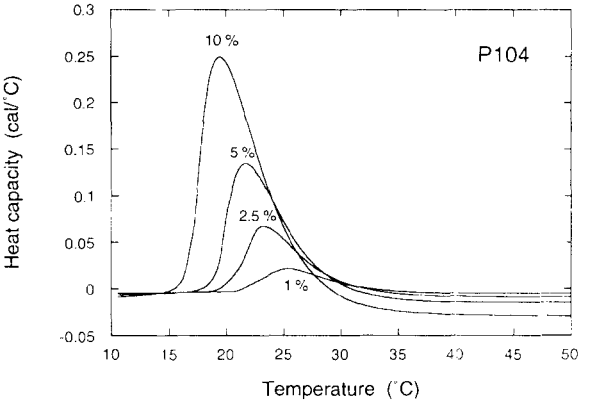

Fig. 6. Differential scanning calorimetry curves for Pluronic P104 aqueous solutions at various copolymer concentrations; the endothermic peak is indicative of micelle formation. (Adapted from Ref. [31].)

copolymer molecules before and after micellization. The standard state enthalpy change is defined for transfer of 1 mol of copolymers from the ideally dilute solution to the solvated micellar state. In the ideally dilute solution, copolymer segments interact only with the solvent, whereas in real solutions segments also interact with each other, and this may cause discrepancies between micellization enthalpies obtained from DSC and those derived from an analysis similar to that of Alexandridis et al. [28]. It has also been reported by Hiemenz [41] that ΔH° values calculated by a micellization thermodynamics model generally give poor agreement with those determined calorimetrically, at least for ionic surfactants.

From a rather limited set of data (Pluronics P123, F127, and P104), Wanka et al. [30] observed no proportionality between the DSC enthalpy values and the size of the PEO block of the molecules, but noted that, to a first approximation, there was proportionality between these values and the number of PO segments. They concluded from this that the transition was probably due to the dehydration or "melting" of the PO segments. Similar trends were observed in the ΔH° data of Alexandridis et al. [28], although a weak effect of PEO block size on ΔH° was apparent from the latter data set. For Pluronic copolymers with the same size hydrophobic (PPO) block and varying size hydrophilic (PEO) block (i.e. P103, P104,

P105, and F108), ΔH° decreased by approximately 15% as the number of EO segments increased from 2×7 to 2×132. For Pluronic copolymers with the same size hydrophilic (PEO) block and varying size hydrophobic (PPO) block (i.e. P65, P84, and P123), ΔH° increased by approximately 100% as the number of PO segments increased from 30 to 70. The PPO effect was more significant, leading to the conclusion that PPO is mainly responsible for the micellization of PEO–PPO–PEO copolymers in water. DSC was also used by Beezer et al. [53] and Mitchard et al. [54] to study PEO–PPO–PEO block copolymer aqueous solutions. The observed "phase transitions" were in the 100–300 kJ mol^{-1} range and were initially thought to result from changes in the polymer solvation as the temperature changed. Beezer et al. [53] and Mitchard et al. [54] claimed that, at the concentration used (5 g l^{-1}), only unimers were present in solution. In a more recent paper from the same group, however, Armstrong et al. [52] concluded that the observed enthalpy change is indicative of an aggregation process, accompanied by desolvation and change in conformation of the hydrophobe. Although direct comparison between the calorimetry ΔH values of Refs. [52]–[54] and the ΔH° of Ref. [28] cannot be made as the copolymers used were not the same, the data of the latter paper strongly suggest that the micellization process is the major contributor to the calorimetrically-observed enthalpy change.

4.2. *Effect of copolymer composition and molecular weight on micellization thermodynamics*

Free energies of micellization per mol of Pluronic copolymer in solution, ΔG° (calculated at the CMT for the various copolymers at different solution concentrations), exhibit some scatter when plotted as a function of copolymer molecular weight, but they do indicate a tendency for higher molecular weight copolymers to have more negative free energies of micellization [28]. The ΔG° data collapse into a single smooth curve, independent of the copolymer composition ratio PPO/PEO, when normalized with respect to the total number of monomer segments in the polymer, $N_{EO} + N_{PO}$, as shown in Fig. 7 [28]. It can be seen clearly that lower molecular weight, more hydrophobic Pluronics yield more negative ΔG° values per monomer segment. The dependence of the thermodynamic parameters ΔH° and ΔG° on the PPO/PEO composition ratio was also examined. The normalized ΔH° (expressed in kJ mol^{-1} of average monomer segment) approached zero as the PPO/PEO ratio went to zero [28]. It can thus be inferred that the micellization process is dominated by the PPO (hydrophobic) part of the copolymer. A similar trend was observed by Armstrong et al. [52] based on DSC enthalpy changes of ICI Poloxamer solutions, and by Williams et al. [55] using the increment in apparent molar volume on "thermal transition" of PolySciences PEO–PPO copolymers as a function of PPO/PEO. The fact that the normalized ΔH° values are approximately the same for Pluronic copolymers of the same PPO/PEO composition ratio and different molecular weights would indicate that the micellization enthalpy per monomer segment is independent of molecular weight.

In contrast to the trend of decreasing ΔG° with increasing Pluronic molecular weight, there is no definite dependence of ΔH° on molecular weight over the range covered in the study of Alexandridis et al. [28]. The ΔH° data presented in Ref. [28] revealed two main groups of copolymers: the relatively hydrophobic Pluronics P103, P104, P105,

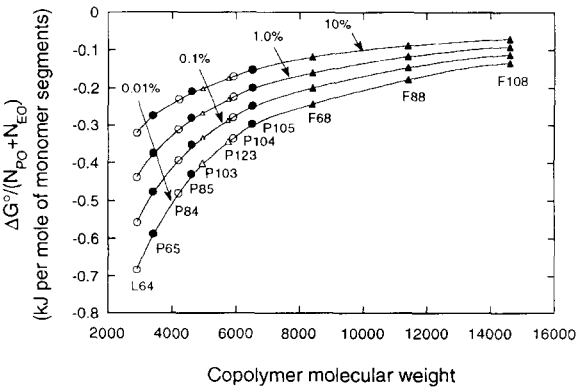

Fig. 7. Effect of PEO–PPO–PEO copolymer molecular weight on the free energies of micellization for various copolymer concentrations expressed as $\Delta G^\circ/(N_{EO} + N_{PO})$ (kJ mol^{-1} of monomer segments). (Reprinted with permission from Ref. [28]; copyright American Chemical Society, 1994.)

and P123 with ΔH° in the 300–350 kJ mol^{-1} range, and the relatively hydrophilic copolymers L64, P65, P84, and P85 with ΔH° in the 180–230 kJ mol^{-1} range: ΔH° for the other four copolymers ranged between 170 and 270 kJ mol^{-1}. A plot of ΔG° of micellization (expressed in kJ mol^{-1} of average monomer segment) as a function of PPO/PEO showed the ΔG°/segment values approaching zero as the PPO/PEO ratio went to zero [28]. The segment free energy, however, decreased (became more negative) with a decrease in molecular weight for PEO–PPO–PEO copolymers having the same PPO/PEO ratio. In a different investigation, Reddy et al. [26] estimated the ΔG° of micellization at -20 kJ mol^{-1} and the ΔH° of micellization at 200 kJ mol^{-1} for a solution of purified Pluronic L64, utilizing ln(CMC) vs. $1/T$ data (only three data points, though). The same group [40] reported the ΔH° of micellization at 316 ± 20 kJ mol^{-1} for a solution of purified F127 (from ln (concentration) vs. $1/T_{CMT}$ data). These values vary by approximately 20% from $\Delta G^{\circ} = -24.5$ kJ mol^{-1}, and $\Delta H^{\circ} = 230$ kJ mol^{-1} for L64 and $\Delta H^{\circ} = 253$ for F127 reported in Ref. [28].

5. Structure of block copolymer micelles

5.1. Aggregation number, micelle size and shape

The association of PEO–PPO–PEO block copolymers into micelles and the structure of these micelles have been investigated by many researchers [21,26–30,37,40,56–70]. We present below information on micelles formed by Pluronics L64, P85, F88, F68, and F127 PEO–PPO–PEO block copolymers, for which a considerable number of studies have been published. Significant information has been obtained from light and neutron scattering studies. In general, the unimer size is found to be approximately 1 nm and the micelle size 10 nm, independent of copolymer concentration (although, the concentrations used were usually high (above approximately 2%) to allow good signal-to-noise ratio in the scattering experiments). The effect of temperature is interesting: an increase in the aggregation number with temperature has been observed, while the micellar radius remains constant. The conclusions are complicated by the rather broad CMT transition, and the fact that dynamic light scattering detects the micelle hydrodynamic radius which includes the water hydrating the EO segments.

Pluronic L64 showed detectable aggregates at 25 °C only at concentrations above approximately 6%; the micelle size increased with concentration (10 nm at 8%–12.5 nm at 20%) and exhibited significant polydispersity, probably indicating a multiple association process [29]. At 35 °C, however, essentially invariant values for the hydrodynamic radius were found over a wide concentration range and the micelles were monodisperse; these systems are more likely represented by a closed association model [29]. Zhou and Chu [56] found that micellar molecular weight increased exponentially with increasing temperature; composition heterogeneity (presence of hydrophobic impurities) caused strong angular asymmetry of scattered light by L64 copolymer solutions. The mode of association of a purified L64 sample in aqueous solution has been examined by Reddy et al. [26]; association at 34.5 and 40 °C was described by a cooperative association model which assumes aggregate growth by stepwise addition of unimers; note that this is in contrast to the results reported by Al-Saden et al. [29]. Almgren et al. [58] calculated (from static light scattering data) the aggregation numbers of L64 at the temperatures 21.0, 25.9, 40.0, and 60.0 °C to be 2, 4, 19, and 85 respectively, indicating a smooth increase with temperature. More recently, the effect of temperature in aqueous solutions of Pluronic L64 was examined by means of viscosity, sedimentation, scattering and sound velocity measurements [67]. The micelles grew large, particularly at temperatures near the cloud point. The viscosity data for L64 were analyzed to estimate various parameters, including the hydrated micellar volume, hydration number, hydrodynamic radius, etc.

Dynamic light scattering experiments in Pluronic P85 solutions indicated the coexistence of unimers (hydrodynamic radius 1.8 nm), micelles (hydrodynamic radius 8 nm), and micellar aggregates, at copolymer concentrations less than 10% and at low temperatures (25 °C) [27]. Micelles

were formed at a copolymer concentration of approximately 5% at 25°C; at temperatures of 40°C and higher, micelles were present at all the concentrations studied ($C > 0.3\%$). The hydrodynamic radius of the micelles (calculated at infinite dilution) was approximately constant (8 nm) over the temperature range 15–50°C (aggregation number 20–40). At finite concentrations the apparent micellar radius increased with increasing temperature. The hard-sphere radius of a copolymer molecule of $M_w = 4500$ would be 1.15 nm; thus, from the 1.8 nm radius observed experimentally one may conclude that the unimer is highly compact, possibly with the PEO chains forming a tight shell around the non-hydrated PPO core [27]. Intrinsic viscosity measurements (capillary viscometry) were made on dilute P85 solutions in order to obtain more information on the molecular dimensions. The intrinsic viscosity decreased from 16 ml g^{-1} at 15°C to 6.5 ml g^{-1} at 50°C. The intrinsic viscosity of 6.5 ml g^{-1} at 50°C suggested a very compact particle (although with some dissymmetry and/or solvation); the radius of gyration, R_g, was estimated at 8.3 nm.

Values for the hydrodynamic radii of the micellar component from self-diffusion coefficients (measured by pulsed-field-gradient NMR and extrapolated to infinite dilution) varied between 6.2 and 9.0 nm in the temperature range 21.3–35.7°C, with an average value of 7.7 nm. This variation with temperature contradicted the constant micelle radius detected using dynamic light scattering. This was possibly the result of polydispersity, since the number-average quantity obtained with NMR would be very sensitive to even small amounts of monomer [27]; the difference between the hydrodynamic radii determined from pulsed field gradient (PFG) NMR and dynamic light scattering was smaller at the higher temperatures at which the suspension is nearly monodisperse. The self-diffusion of Pluronic P85 copolymer in aqueous solution was investigated with PFG-NMR [65,66]. The hydrodynamic radii of the unimer and the micelles were determined to be 1.5 and 4.5 nm, respectively, and found to be independent of temperature and concentration in the concentration range between 1 and 10%. Mortensen and co-workers [61,62] studied the structure of P85 aqueous solutions using neutron scattering. The radius of gyration of the free copolymer was 1.7 nm. The micellar sizes (micelle core radius and hard-sphere interaction radius) appeared to be independent of polymer concentration, but showed a small temperature dependance reflecting changes in aggregation number. The micelle core radius and hard-sphere interaction radius were 3.8 and 6.0 nm at 20°C, respectively, and increased to 5.1 and 7.5 nm at 50°C; the aggregation number was 37 at 20°C, increasing to 78 at 40°C [64].

Brown et al. [57] and Mortensen and Brown [63] published studies comparing the Pluronic PEO–PPO–PEO copolymers P85, F87, and F88. Relaxation time distributions obtained by Laplace inversion of the dynamic light scatting (DLS) correlation functions demonstrated complex states of aggregation in solution [57]. Unimer, micelles, and larger aggregates coexisted in proportions that depended strongly on temperature and concentration, as seen in Fig. 8 for P85 solutions [27]. The unimers had hydrodynamic radii in the size range 1.5–3.0 nm; the micelle radii were 8–13 nm (in sequence of increasing PEO block length), whereas the radii of the clusters were greater than 80 nm. The micelle aggregation number for F88 was 17 at 40°C, and the hydrodynamic radii 13 and 10.5 nm at 40 and 50°C, respectively. Molecular weights, gyration radii, etc., could not be determined from static light scattering measurements owing to the highly polydisperse character of the solutions. The inverse osmotic compressibility was evaluated from the absolute scattering intensity at zero angle, providing a measure of the relative strengths of solute/solvent and solute/solute interactions; formation of micelles and aggregates was consistent with low values of the inverse osmotic compressibility. Pluronics P85, F87, and F88 had approximately the same tendency for micelle formation when compared at the same molar concentration; for the same weight concentration, P85 formed micelles more readily [57]. Mortensen and Brown [63] found that the critical micellization temperature values of Pluronics L81, P85, P87 and F88 fell on a common line when plotted against the concentration of PPO in solution; it thus appeared that the PPO concentration was the relevant parameter in the

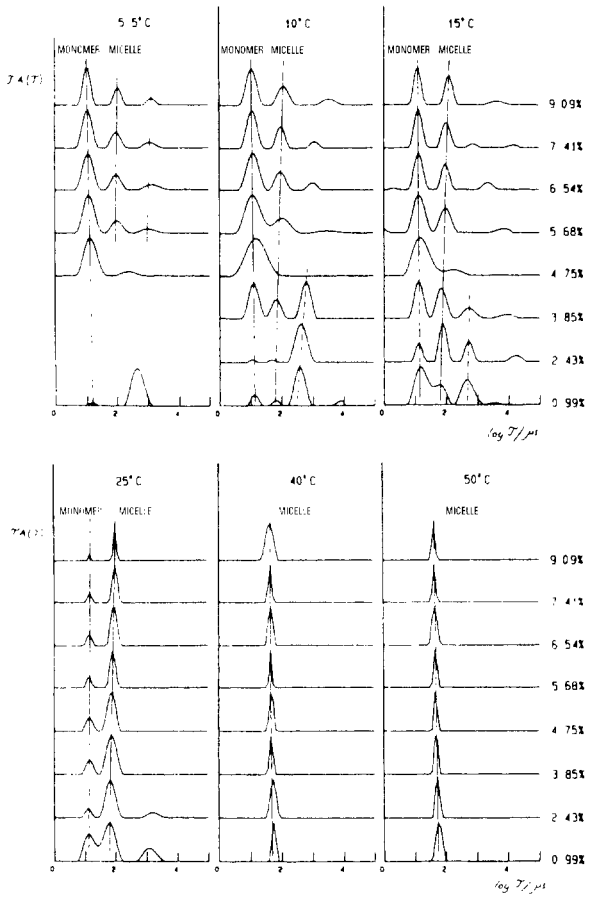

Fig. 8. Relaxation time distributions obtained by Laplace inversion of dynamic light scattering data, $\tau A(\tau)$ vs. $\log(\tau/\mu s)$, for Pluronic P85 at low concentrations (<10%) and at temperatures between 5 and 50 °C ($A(\tau)$ is the autocorrelation function). Peaks attributed to unimer and micelles are indicated, in addition to the peaks at low concentrations which probably reflect clusters of diblock contaminant. (Reprinted with permission from Ref. [27]; copyright American Chemical Society, 1991.)

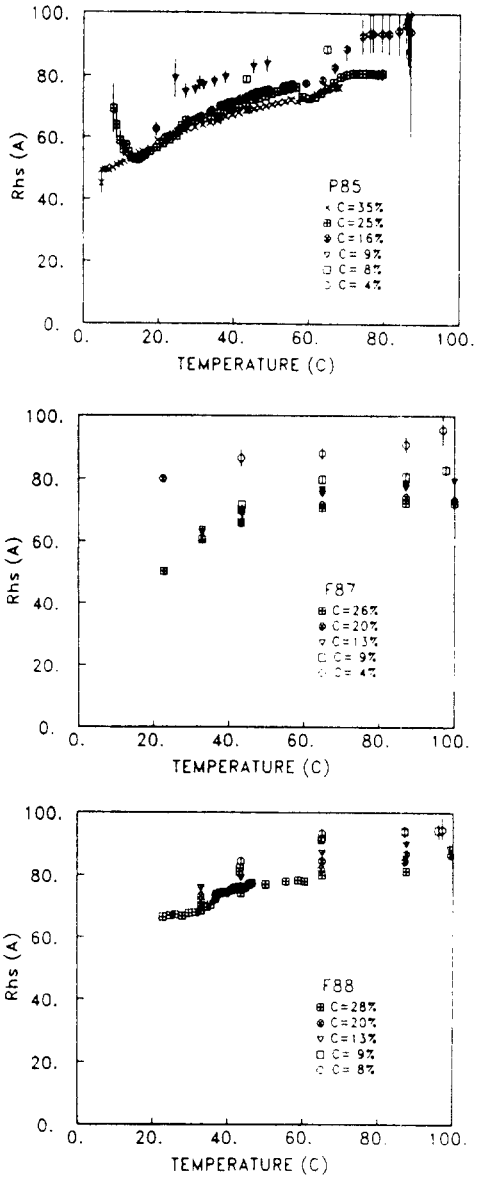

Fig. 9. Hard-sphere interaction radius, R_{hs}, for Pluronic P85, P87, and F88 PEO–PPO–PEO copolymers, obtained by fitting the hard-sphere Percus–Yevick model to experimental neutron scattering data; the radii are plotted as a function of temperature for different copolymer concentrations. (Reprinted with permission from Ref. [63]; copyright American Chemical Society, 1993.)

determination of the CMT. Pluronic L81 formed aggregates at temperatures below the common curve, presumably due to the significantly greater hydrophobic nature of L81 (L81 contains 90% PPO); there was also some deviation from the curve for P85 at low PPO concentrations.

The hard-sphere interaction radius, R_{hs}, for Pluronics P85, P87 and F88, obtained by fitting to the experimental scattering data, is shown in Fig. 9 [63]. The radii are plotted as a function of temperature for different copolymer concentrations. The micellar core radius, R_c, and to some extent also the hard-sphere interaction radius, R_{hs},

appeared to be essentially independent of copolymer concentration but showed a significant increase with temperature. The difference between R_c and R_{hs} remained practically unaffected by the temperature. When R_c was plotted against reduced temperature $T-T_{CMT}$, the data for solutions of P85, P87, and F88 followed a common master curve. A double logarithmic plot of R_c vs. $T-T_{CMC}$ gave the empirical scaling relation $R_c \approx (T-T_{CMT})^{0.2}$ as seen in Fig. 10 [63]. The aggregation number was very small, close to T_{CMT}, and increased continuously following a $N \approx (T-T_{CMT})^{0.6}$ relationship to $N \approx 200$ at the highest temperature, where spherical micellar aggregates were present. From the hard-sphere data analysis, it appears that the main difference between P85, P87, and F88 micelles at a given temperature is the size of the micelles; the larger the PEO block, the smaller the core and the aggregation number [63]. The dependence of the core radius and the aggregation number on the degree of polymerization of both EO and PO [63] contradicted the Halperin [71] star model of polymeric micelles, which was recently shown to be valid for the system PEO–PS–PEO [72]. The relationship of increasing micellar core with decreasing number of EO segments would lead to a limitation in the formation of spherical micelles; this would happen if the number of EO segments were so small that the core radius extended the length of a stretched PPO chain. Extrapolation of the core radii data for Pluronics P85, F87, and F88 to the number of EO segments corresponding to L81 would lead to a value for the core approaching or exceeding the maximum value given by the length of a fully extended PPO chain; this is probably the reason why Pluronic L81 does not form spherical micellar aggregates [63].

Static and dynamic light scattering experiments on Pluronic F68 aqueous solutions revealed three temperature regions, those of unimer, transition, and micelle [21]. The apparent hydrodynamic radii of F68 solutions at three different copolymer concentrations are presented in Fig. 11(a) [21]. A transition corresponding to the CMT was observed; below the CMT, low scattering intensity and small particle size (2.3 nm) were detected,

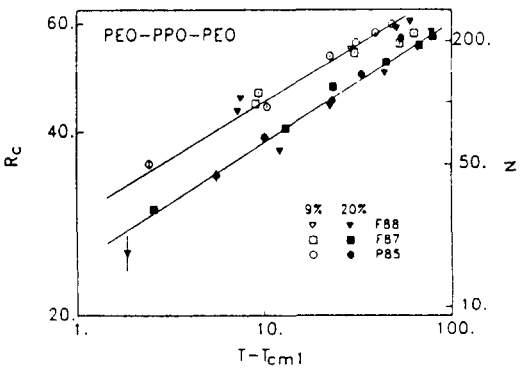

Fig. 10. Double logarithmic plot of R_c vs. reduced temperature, $T-T_{CMC}$ (data shown for 9% and 20% aqueous solutions of Pluronic P85, F87, and F88). (Reprinted with permission from Ref. [63]; copyright American Chemical Society, 1993.)

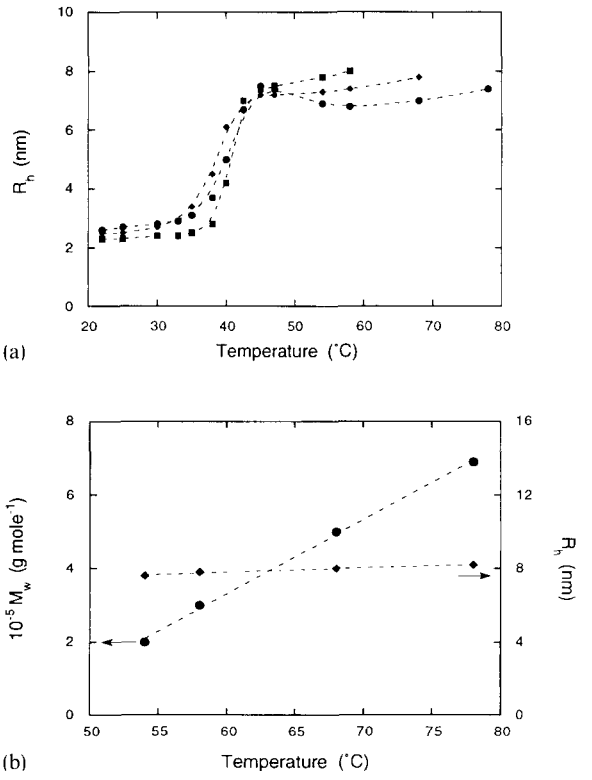

Fig. 11. (a) Temperature dependence of apparent hydrodynamic radius of Pluronic F68 solutions at three different concentrations: ◆, 51.7 mg ml^{-1}; ●, 25.0 mg ml^{-1}; ■, 12.5 mg ml^{-1}. (b) Linear increase of F68 micellar weights with increasing temperature, with the hydrodynamic radius of the micelles remaining approximately constant. (Reprinted with permission from Ref. [21]; copyright Academic Press, 1988.)

showing little temperature dependence. Only unimers were present below the CMT; micelle formation became appreciable above the CMT. In the micelle region, the micellar weights measured were of the order of 10^5 g mol^{-1} (average aggregation number was 65) and increased linearly with temperature, while the hydrodynamic radii of the micelles remained nearly constant (8.0 nm) as seen in Fig. 11(b) [21] (note, however, that Al-Saden et al. [29] reported the average hydrodynamic radius to increase with temperature for a given concentration). Such a dual effect of temperature was interpreted in terms of enhanced dehydration of the micelle corona (consisting mainly of PEO) with temperature [21]. In static light scattering measurements, the scattered light field is a measure of the polarizability difference between the dispersed particle and the surrounding medium, thus providing useful information concerning the "dry" dispersed particles. In the dynamic light scattering experiments, the Brownian motion of the "wet" dispersed particles is monitored to provide size information on the solvated particles. It is well established that dehydration of non-ionic surfactants gradually occurs with increasing temperature, which results in an enhanced tendency to separate from the solvent environment and, consequently, in an increase in the aggregation number. Such a dual effect of temperature increase on an increased aggregation number and a decreased micellar hydration makes it possible for the hydrodynamic radius of PEO–PPO–PEO copolymer micelles to remain almost independent of temperature [21].

The hydrodynamic radii of micelles formed by Pluronic F127 in water, as calculated from diffusion (QELS) data at the CMC, remained constant at 10.2 nm, over the 35–45 °C temperature range [73]. Viscometric studies, however, showed a progressive dehydration of the micelles with temperature increase; the aggregation number was 3 at 35 °C, 9 at 40 °C, and 12 at 45 °C [73]. Malmsten and Lindman [59] used NMR to study diffusion of molecules in F127 solutions. The diffusion of the polymer molecules was slow ($D_p = 10^{-11}$–10^{-12} m^2 s^{-1}) and decreased with increasing copolymer concentration (roughly as $D_p \approx c^{-1}$) up to 20 wt.%; the diffusion coefficient of water was $D_w = 10^{-9}$ m^2 s^{-1} [59]. Water self-diffusion decreased monotonically with increasing copolymer concentration, giving $D/D_0 = 0.5$ at 40 wt.%. The decrease in D/D_0 with increasing copolymer concentration could be reproduced by taking into account the obstruction due to excluded volume and the hydration of the polymer molecules. The analysis yielded that somewhere between two and five water molecules per EO segment were perturbed. The water diffusion increased with temperature. The data of Malmsten and Lindman [59,60] are consistent with a gradual dehydration of the polymer molecules with increasing temperature, and are in agreement with those of Attwood et al. [73]. Such a dehydration, however, did not correlate with the occurrence of the gel region [60].

5.2. *Micelle microenvironment*

Fluorescence spectroscopy techniques have been developed and optimized over the past 15 years for the study of colloidal solutions, and many fluorescent molecules are now available for probing structural information in such systems [34,77]. Pyrene, amongst others, is a well-characterized polarity-sensitive probe. The pyrene fluorescence emission spectrum consists mainly of five bands referred to as, I_1, I_2, ..., I_5, from shorter to longer wavelengths. The I_1/I_3 intensity ratio of this vibrational fine structure depends strongly on the polarity of the medium; the larger the ratio, the more polar the medium. Electronically excited pyrene is a reporter of the average micropolarity of the environment it visits during its lifetime (≈ 300 ns), rendering pyrene attractive for studying restricted microenvironments such as micellar systems [34,77].

Alexandridis and co-workers [37,70,76] used pyrene to probe the micropolarity in Pluronic copolymer solutions, by conducting a systematic investigation of the variation of the pyrene fluorescence emission intensity ratio I_1/I_3 in different media as a function of temperature. Specifically, studies were conducted in water, organic solvents, bulk PEO and PPO homopolymers, and aqueous solutions of PEO–PPO–PEO copolymers. A sharp decrease in I_1/I_3 was observed for PEO–PPO–PEO triblock copolymer solutions, at temperatures characteristic of each polymer, followed

by a less dramatic linear decrease as the temperature was further increased (see Figure 12(a)). This sharp decrease is attributed to the formation of micelles with a well-defined hydrophobic core into which pyrene partitions preferentially. The temperature dependence of the I_1/I_3 intensity ratio can be used for the determination of the CMT [37], as with the I_1/I_3 vs. concentration plots in the determination of the CMC in surfactant systems [34]. The smoother linear decrease observed at temperatures higher than the CMT reflects a less polar microenvironment with increasing temperature. This was attributed to a temperature-induced change in the solution micropolarity [70]. The influence of molecular weight on the micropolarity afforded by copolymer micellar solutions is depicted in Fig. 12(a) for a series of Pluronic copolymers (P105, P85, P65) with the same PPO/PEO composition ratio (50%). The highest molecular weight P105 exhibited the lowest CMT, in accordance with the findings of Ref. [28]. At temperatures higher than the CMT, the I_1/I_3 ratios decreased linearly with increasing temperature for all copolymers, but their values remained in the order: I_1/I_3 (P65) > I_1/I_3 (P85) > I_1/I_3 (P105). This is an indication that micelles assembled from higher-molecular-weight Pluronics (maintaining constant PPO/PEO copolymer composition) exhibit more hydrophobic microdomains [70]. In addition to probing the microenvironment, time-resolved fluorescence quenching from pyrene has been used to determine the aggregation number of PEO–PPO–PEO micelles [70,75].

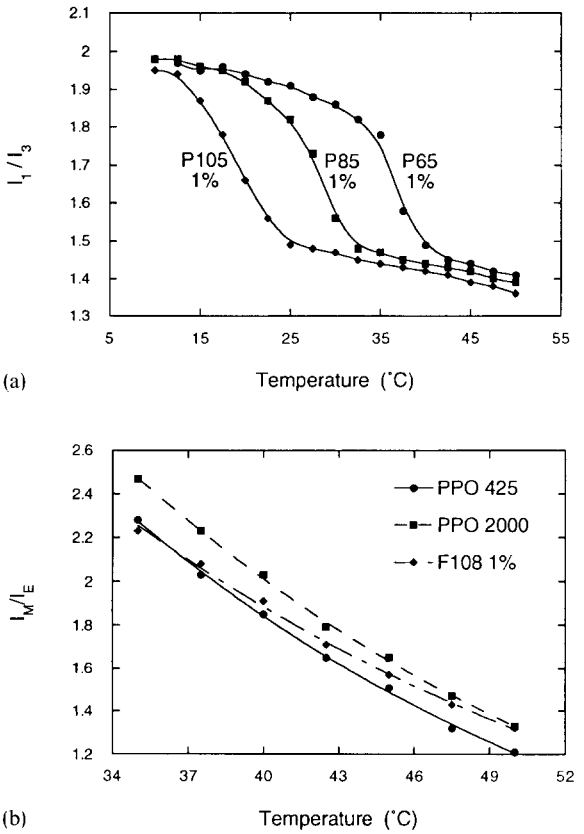

Fig. 12. (a) Micropolarity in PEO–PPO–PEO copolymer solutions: pyrene fluorescence emission intensity ratio (I_1/I_3) as a function of temperature for 1% aqueous solutions of Pluronics P105, P85, and P65. (Adapted from Ref. [76]; copyright Massachusetts Institute of Technology, 1994.) (b) Microviscosity in PEO–PPO–PEO copolymer micelles: dipyme fluorescence emission monomer/excimer intensity ratio (I_M/I_E) as a function of temperature for Pluronic F108 micelles; also shown in the same graph for comparison purposes are data for bulk PPO homopolymer. (Adapted from Ref. [79].)

The microviscosity in the interior of block copolymer micelles can be probed using the hydrophobic molecule bis(1-pyrenylmethyl)ether (dipyme) that exhibits intramolecular excimer fluorescence (intensity I_E) in competition with fluorescence from the locally excited pyrene chromophore ("monomer" emission, intensity I_M; I_5 is used here to represent I_M) [78]. The extent of excimer emission in dipyme depends upon the rate of conformational change, the motion of the pyrene segments of dipyme being restricted by the local friction imposed by the environment. As a consequence, the intensity ratio I_M/I_E provides a measure of the "microviscosity" of its environment (the larger the I_M/I_E ratio, the more viscous the environment in which the probe is located), and is a particularly powerful means of monitoring changes in microviscosity as the system is subjected to external stimuli [78].

Qualitative changes in the microviscosity experienced by dipyme are reported by Nivaggioli et al. [79] for PPO homopolymers and PEO–PPO–PEO copolymer micellar solutions, as a function of a copolymer composition and sample temperature. Values of the monomer/excimer intensity ratio (I_M/I_E) of dipyme in bulk PPO homopolymers and Pluronic F108 micelles are

shown in Fig. 12(b) [79]. I_M/I_E data are reported for the 35–50°C temperature range, so that micelles are present in which dipyme can be solubilized (the solubility of dipyme in water is very limited). Microviscosity decreased with temperature for all the systems studied; higher microviscosity values were observed for the higher M_w PPO. The I_M/I_E values for the F108 micelles are comparable with those for bulk PPO, suggesting that the environment in which dipyme is located is similar to bulk PPO. Note that the microviscosity experienced by dipyme in the interior of F108 micelles appears to be similar to that sensed in low M_w (725) PPO at 35°C, while it exceeds the microviscosity in high M_2 (2000) PPO at 50°C. This could be an indication that the micelle core becomes more compact as the temperature increases. Such an observation can be related to the fact that the aggregation number of Pluronic copolymer micelles increases with temperature, while the hydrodynamic radius remains approximately constant (see Section 5.1). A semilog plot of I_M/I_E vs. temperature can be fitted to a linear relationship [79]; activation energy (E_a) values for the microviscosity experienced by dipyme can be estimated from such a plot. Increase of the copolymer molecular weight at constant PPO/PEO composition, and increase of the PPO block size for constant PEO block size, resulted in increasing microviscosity and activation energies. The effect of PEO block on micelle microviscosity was less significant.

The hydration and microviscosity in the micellar solutions and gels formed by Pluronic F127 have been studied using the fluorescent probe molecules pyrene and 8-anilino-1-naphthalene sulfonic acid [74]: the results indicated that microviscosity decreases with increasing temperature. Recently, Nakashima et al. [80] reported fluorescence anisotropy data from octadecyl rhodamine B in Pluronic F68 PEO–PPO–PEO micelles; the microviscosity of the latter was estimated from these measurements. The microviscosity increased from 1.9 cP at 20°C to 16 cP at 40°C; this increase was attributed to a conformational change of the micelles from a loosely coiled aggregate to a more compact structure. Note however, that octadecyl rhodamine B is a cationic amphiphilic molecule that will most likely associate with the micelle corona, thus complicating the microviscosity studies.

5.3. Phase diagram

The phase behavior of PEO–PPO–PEO triblock copolymers dissolved in water has been studied by Mortensen and co-workers using small-angle neutron scattering and dynamic light scattering [61,63,64]. The structural properties have been studied as a function of polymer concentration and temperature for a series of Pluronic copolymers with PPO blocks of constant size and PEO blocks of varying size. At low temperature ($T \leq 15$ °C) and low polymer concentrations, the unimers were fully dissolved gaussian chains with radius $R_g = 1.7$ nm. Close to ambient temperature, the hydrophobic nature of PPO caused aggregation of the polymers into spherical micelles with core sizes of the order of 4–5 nm, somewhat temperature dependent. According to the data analysis, the core size increased with decreasing PEO block size and with increasing temperature. The copolymer with the largest PEO block aggregated in micelles with a core diameter which, within the whole temperature regime, was smaller than the length of a stretched PPO chain. Micelles formed by copolymers of intermediate PEO size had a core diameter which at high temperature approached the size of a fully stretched PPO chain, thus causing an abrupt change from a spherical to a rod-like structure (as observed both by neutron scattering and depolarized light scattering). It appeared from the hard-sphere data analysis that the micelle-forming polymers could all be scaled to a common phase behavior where the critical micellization temperature is determined by the PPO concentration, whereas the crystallization (gelation) temperature is determined by the total copolymer concentration [63]. The concentration of micelles increased roughly linearly with temperature until either a saturation was reached (where all polymers were part of a micelle) or the volume density of micelles was so high that they "locked" into a crystalline structure of hard spheres. In the 60–70 °C temperature range, the micellar structure changed from spherical form to prolate ellipsoid, leading to a

decreasing intermicelle interaction. At high copolymer concentration this caused melting of the cubic lattice and led successively to the formation of a rod-like structure with hexagonal symmetry. Large aggregates of PEO–PPO–PEO copolymers ordered in lamellae structure were formed close to 95°C, leading to an opaque suspension [64].

The phase diagram of Pluronic P85 PEO–PPO–PEO copolymer in water is presented in Fig. 13, in which the concentration–temperature regions where the different aggregates (discussed in the previous paragraph) exist are also depicted [61]. The micellization boundary (phase diagram) for a number of Pluronic PEO–PPO–PEO copolymers in aqueous solutions is shown in Fig. 14 [76] (the CMC–CMT data are extracted from Ref. [28]). The free polymer (unimer) is in solution at copolymer concentrations and temperatures lower than the CMC–CMT boundary; micelles in equilibrium with unimers are present above the boundary. Recently, Wanka et al. [69] reported the phase diagrams of several PEO–PPO–PEO copolymers in water. Unimer, micellar, cubic (gel), hexagonal, and lamellar phases were observed;

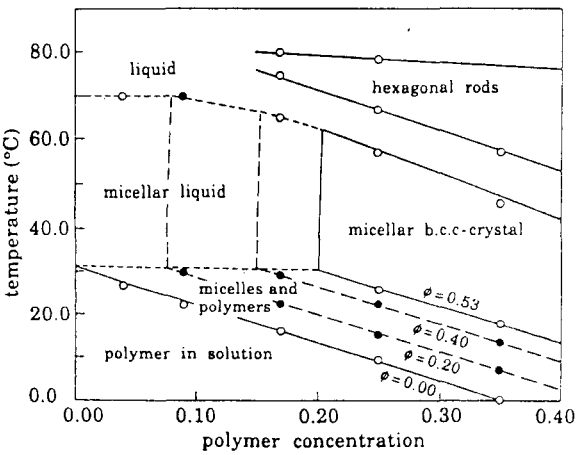

Fig. 13. Phase diagram of aqueous Pluronic P85 solution, showing the fully dissolved polymers (unimers) at low temperatures and concentrations, the CMC–CMT line ($\phi=0$), the $\phi_c=0.53$ transition to b.c.c. micellar crystal, and the high-temperature hexagonal phase (ϕ is the hard-sphere micelle volume fraction). At $T\approx 60$°C a liquid phase appears between the crystalline b.c.c. and hexagonal phases. (Reprinted with permission from Ref. [61]; copyright European Physical Society, 1992.)

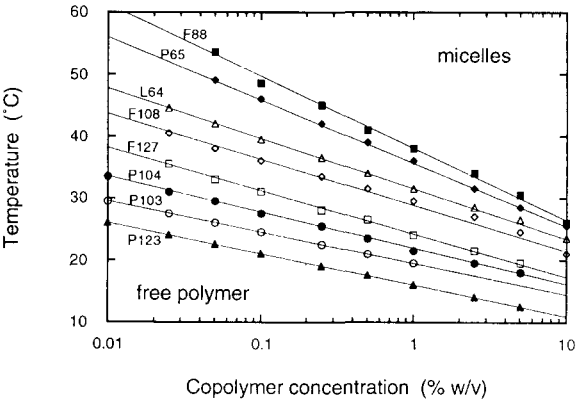

Fig. 14. Phase diagram of aqueous Pluronic PEO–PPO–PEO copolymer solutions, showing the CMC–CMT micellization boundary. The free polymer (unimer) is in solution at copolymer concentrations and temperatures lower than the CMC–CMT boundary; micelles in equilibrium with unimers are present above the boundary. (Reprinted with permission from Ref. [76]; copyright Massachusetts Institute of Technology, 1994.)

their occurrence depended on the copolymer PPO/PEO composition ratio. Copolymers with a small hydrophilic PEO block usually formed a hexagonal phase as the first liquid crystalline mesophase. The lyotropic mesophases exhibited thermotropic behavior: reversible transitions between the different phases occurred with increasing temperature at constant copolymer concentration. The phase behavior of a monoolein-rich (89.5 wt.%) monoglyceride blend based on pine needle oil, Pluronic F127, and water has been investigated by small-angle X-ray diffraction and reported recently by Landh [81]; an extended cubic phase region was observed.

5.4. *Effect of additives on micellization*

The phase behavior of Pluronic L64 PEO–PPO–PEO block copolymer in the presence of various additives was studied by Pandya et al. [67] using cloud point and phenol index (i.e. the amount of phenol added to give a turbid solution) measurements. Addition of electrolytes, having anions and cations of different sizes and polarizabilities, resulted in either an increase or a decrease in cloud point; the effect of salts was discussed in terms of "salting in" and "salting out" and followed the Hofmeister series [67]. The effect of various

non-electrolytes (e.g. hydroxy compounds and amides) on the cloud point of L64 was also examined and discussed in terms of their influence on water structure [67]. The aggregation behavior of Pluronics P85 and L64 in aqueous solution has been investigated in the presence of added salts (KCNS, KI, KBr, KCl and KF) by viscosity, cloud point, light scattering, pulse gradient spin echo NMR, and solubilization measurements [82]. The salts have a strong effect on the cloud point of the PEO–PPO–PEO copolymers. A slight linear increase in cloud point was observed with an increase in copolymer concentration in the case of L64, following an initial decrease up to a copolymer concentration of approximately 2%. KCNS, which is known to increase the cloud point, showed a similar trend in both L64 and P85 solutions; addition of KBr, KCl, and KF decreased the cloud point. A linear change (increase or decrease) in the cloud point with increasing salt concentration was observed. Both Pluronic P85 and L64 formed micelles which increased in size and became elongated in shape when the cloud point was approached. The changes of size and shape of the micelles, revealed by the intrinsic viscosity and rheological properties of the solution, seemed to occur at the same temperature relative to the cloud point, independent of the nature of the salt. The onset of micelle formation was also shifted in the same direction as the cloud point by the salts, but to a lesser degree [82].

The cloud point of Pluronic F68 was reduced by 50 °C when 1.0 M KF was added to the aqueous solution [83]. The size of the unimers and micelles in the solution, as estimated from diffusion coefficients (determined by dynamic light scattering and NMR self-diffusion measurements) or micelle molecular weights (from static light scattering), was similar in the presence and absence of salts, but the growth of the micelles started at a lower temperature (25 °C in 1.0 M KF, 44 °C in water) and continued over a wider temperature range in the salt solution [83]. The influence of temperature on Pluronic F127 micellar size and hydration was less pronounced in the presence of 0.5 mol dm^{-1} NaCl in the aqueous solution [73]. The influence of agarose on the clouding behavior and the diffusion of $EO_{13}PO_{30}EO_{13}$ copolymer, as well as the effect of the copolymer on the gelation properties of agarose were recently reported by Penders et al. [84]. The cloud point of $EO_{13}PO_{30}EO_{13}$ on cooling and the self-diffusion of the copolymer decreased in the presence of agarose gels. The presence of 1.0 M NaSCN suppressed the formation and growth of $EO_{13}PO_{30}EO_{13}$ micelles [84].

The effects of urea on the micellization properties of Pluronic P105 PEO–PPO–PEO copolymer, and on the structure and microenvironment of the micelles were investigated by Alexandridis et al. [85]. CMC and CMT data for Pluronic P105 dissolved in urea/water mixtures (urea concentration: 0, 1, 2, and 4 M) were obtained using a dye solubilization method and corroborated with surface tension, density, and fluorescence spectroscopy experiments. Addition of urea increased the CMC and CMT of the PEO–PPO–PEO copolymer; the effect of urea on the CMT was more pronounced at low copolymer concentrations and diminished at concentrations of approximately 2.5%. The thermodynamic parameters of P105 micelle formation in the presence of urea were estimated using a closed association model; the enthalpy of micellization was positive (endothermic) and decreased upon increasing the urea concentration. The surface activity and the partial specific volume of Pluronic P105 decreased with an increase in the urea concentration, whereas the hydrodynamic radii of the copolymer micelles, determined using dynamic light scattering, remained unaffected by the presence of 4 M urea in the solution. The micropolarity in copolymer solutions in urea/water was probed as a function of temperature using the I_1/I_3 intensity ratio of the pyrene fluorescence emission spectra; a small decrease in the micropolarity of the micelle core was observed in the presence of urea [85].

Sodium dodecyl sulfate (SDS) increased the cloud point of Pluronic L64, which otherwise decreased in the presence of small amounts of electrolytes. The clouding behavior of a mixed L64/SDS system in the absence and presence of salt was discussed by Pandya et al. [67], primarily in terms of electrical charge on the micelle surface. NMR chemical shift measurements and fluorescence quenching have been combined in a study of the aggregation behavior and properties of

Pluronics L64 and F68 in the presence of SDS at 20 and 40°C [86]. While the copolymers did not form micelles at 20°C, they formed mixed micelles with SDS, at SDS concentrations as low as 1 mM. The aggregation numbers obtained from fluorescence quenching studies indicate that about three SDS molecules per copolymer molecule are needed to "glue" together the PPO blocks into a hydrophobic core at 20°C [86]. The micelles formed at low SDS concentrations were small (15 SDS molecules associated with four to five copolymer molecules); the micelles consisted mainly of SDS at high SDS concentrations. L64 formed micelles at 40°C that were large but decreased rapidly in size upon addition of SDS. The ^{13}C chemical shifts for the methyl carbons in the PPO block were indicative of a change from a coiled conformation in small micelles, unimers, as well as in the bulk PPO liquid, to a more extended PPO conformation in the large micelles. The change of the shifts of the individual carbons in the alkyl chain of SDS on addition of the copolymers to SDS micelles followed a similar pattern for both L64 and F68 PEO–PPO–PEO copolymers [86].

Recently, Hecht and Hoffmann [87] reported the influence of SDS on the aggregation behavior of Pluronic F127. For block copolymer solutions in the concentration range of 1–5% and increasing SDS concentration, the light scattering intensity passed through a deep minimum, the electric birefringence passed over a maximum, and the endothermic peak of the DSC signals (due to the micellization of the block copolymer) disappeared. These results indicate that SDS binds to unimers of F127 and thereby suppresses completely the formation of F127 micelles. Approximately six SDS molecules bind to one F127 PEO–PPO–PEO copolymer molecule at saturation. The birefringence data indicated that the F127/SDS complex exists in a more or less extended conformation and not as a coil. The binding of SDS on F127 was also confirmed by surface tension measurements, which showed the surface active block copolymers to be displaced from the air–water interfaces by SDS molecules. The binding of SDS on F127 commenced at a concentration far below the CMC of SDS. Addition of CTAB (*N*-cetyl-*N*,*N*,*N*-trimethylammonium bromide) to F127 solutions decreased the magnitude of the DSC peak, showing that CTAB (a cationic surfactant) also suppresses the micellization of F127. The zwitterionic surfactant C_{14}DMAO (*N*,*N*-dimethyl-1-tetradecanamine-*N*-oxide) suppresses F127 micellization at concentrations ten times above its CMC, suggesting a different mode of association than SDS; maybe, F127 molecules bind to the surface of C_{14}DMAO micelles [87].

6. Modeling of block copolymer micellization and micelle structure

Theories of micelle formation in solutions of block copolymers have been suggested by a number of researchers over the past decade. Leibler et al. [88], Noolandi and Hong [89], Munch and Gast [90], and Nagarajan and Ganesh [91] computed the free energy of micelle formation assuming uniform copolymer segment concentrations in the core and corona regions, respectively. Scaling theories for polymeric micelles with an insoluble core and an extended corona were developed by Halperin [71], Marques [92], Semenov [93], and Zhulina and Birshtein [94]. In a third approach, van Lent and Scheutjens [95], Linse [50,51], and Hurter et al. [48,49] used a self-consistent mean-field theory to determine the detailed segment density profiles within a micelle, making no a priori assumptions as to the locations of the micellar components. The micelle structures determined from this model have been confirmed recently by Monte Carlo simulations (e.g. Wang et al. [96]), and show that the interfacial region between the core and corona of the micelle is diffuse and not sharp as is assumed in the other modeling approaches.

6.1. Phenomenological models

Munch and Gast [90] applied the theory of Leibler et al. [88], which treated micelle formation in mixtures of block copolymers and homopolymers, to describe the micellization of diblock A–B copolymers in solution. The micelle core was assumed to be a melt of B chains, while the corona contained A chains with solvent S. The interaction

between the solvent S and the B segment was described by the χ_{BS} interaction parameter, whereas athermal interactions between the A segment and solvent were assumed ($\chi_{AS}=0$). The energy of a single micelle was expressed as a contribution of the core–solvent interfacial energy, the energy due to deformation of the copolymer chains in the micelle, and the free energy of mixing of solvent molecules with the A monomers in the corona (ϕ_0: volume fraction of A in the corona). The total free energy of the system included the energy of the micelles, the free energy of mixing individual diblock copolymers (unimers) with solvent molecules (ϕ_1: volume fraction of copolymers outside the micelles), and an energy contribution arising from the translational entropy of the gas of micelles. The total free energy was minimized with respect to the micelle aggregation number p, and the volume fractions ϕ_1 and ϕ_0. One useful feature of the theory of Leibler et al. [88] is that, for a high degree of incompatibility between B and S, the free energy minimization with respect to ϕ_1 results in an analytical estimate for CMC as $\phi_1 \rightarrow 0$ [88,90]:

$$\phi_1 \approx \exp(f/kT + N - \chi_{BS}N_B) \quad (13)$$

where f/kT is the energy per copolymer chain in an isolated micelle, N is the total number of segments in the copolymer molecule, N_B is the number of B (core) segments, and $\chi_{BS}N_B$ is the total effective interaction per chain (since the A chain is in an athermal environment). The leading order terms in the f/kT expression are [90]

$$f/kT \approx (6\pi^2 N_B)^{1/6}(\chi_{BS}N_B)^{1/2}p^{-1/3} + N(1+N_B/N_A)^{-1}(1-\phi_o)\phi_o^{-1}\ln(1-\phi_o) \quad (14)$$

The first term on the right-hand-side of Eq. (14) arises from the energy required to form the micelle core–solvent interface and opposes the formation of micelles, whereas the second term, which originates from the configurational entropy of mixing solvent molecules with A segments in the corona, favors micellization. As χ_{AS} was assumed to be zero, no effect of block A on micellization could be observed in the model of Munch and Gast, other than the configurational entropy of mixing of solvent molecules with A monomers in the corona. The micellization model of Nagarajan and Ganesh [91] took into account A–solvent interactions; however, this was at the expense of an analytical expression for ϕ_{CMC}.

In the micellization theory developed by Nagarajan and Ganesh [91] the micelles were also assumed to have a completely segregated core region, consisting of only the B block, and a corona region consisting of the solvent S and the solvent-compatible A block. The free energy of micellization was expressed in terms of changes in the state of dilution of blocks A and B, changes in the state of deformation of blocks A and B, localization of the copolymer molecules at the micelle interface, and formation of the micellar core–solvent interface. The hydrophobic interactions, which strongly influence the micellization in water as discussed in Section 4, were implicitly accounted for in the experimentally determined χ values used for the PEO–water and PPO–water interaction free energy terms. The micellization parameters were obtained from minimization of the free energy expression with respect to the radius of the micelle core and the corona thickness. The most important contribution favoring micellization arises from the change in state of dilution of block B as it goes from solvent S into the micelle core. Note that the mutual incompatibility of blocks A and B is also essential for micellization, otherwise the incompatibility between the solvent and polymer blocks will give rise to macroscopic phase separation; the incompatibility of blocks A and B was implicitly taken into account by the completely segregated core structure assumed for the micelle. The most important contribution opposing micellization originates from the formation of the micelle core–solvent interface. The optimal aggregation number is determined primarily by balancing the free energy contributions due to change in state of dilution and deformation of the A (more important in the case of the PEO–PPO–water system) and B blocks, favoring low aggregation numbers, and the free energy contributions due to formation of the micelle core–solvent interface that favor high aggregation numbers. The theory of Nagarajan and Ganesh, developed for diblock copolymers, succeeds in predicting qualitatively the contribu-

tions of the copolymer composition and molecular weight on the micellization of triblock copolymers. The trends are the same in both theory and experiment, although the theory overpredicts the experimentally obtained free energies of micellization by a factor of eight [76], resulting in unrealistically low CMC values. Part of the numerical discrepancy could be eliminated by adding extra terms in the expression for the free energy of micellization, to account for the entropy penalty involved in joining two AB diblock copolymer molecules to create a AB_2A triblock, and in having loops in the micelle core.

Prochazka et al. [97] modified Nagarajan's model to treat the association of A–B–A triblock copolymers in solvents selective for A blocks, by introducing two additional terms into the free energy expression discussed above. These terms accounted for the reduction in entropy due to loop formation of the middle (B) block, and the localization of the two A–B joints of the copolymer at the interface between the core and the corona of the micelle. This modification resulted in less negative ΔG° values (in the correct direction with respect to agreement between experiment and theory), but the decrease in the absolute value of the predicted ΔG° was approximately 10%, not enough to account for the eight-fold overprediction of the experimental ΔG° values. A comparison of the model calculations by Nagarajan and Ganesh [91] for a diblock copolymer with the results of Prochazka et al. [97] obtained for a triblock copolymer (of the same molecular weight and composition as the diblock) showed the aggregation number of the diblock copolymer micelles to be three to five times higher than that for the triblock micelles. Linse [50,51] concluded, using a mean-field lattice micellization model, that there is a five-fold increase in CMC and a four-fold decrease in aggregation number on going from a di- to a triblock PEO–PPO copolymer. Prochazka et al. [97] also made an interesting observation regarding the effect of the deformation energy contribution on the model ΔG° expression: model calculations using the deformation energy terms of Nagarajan and Leibler et al. [88] resulted in different aggregation numbers, although both terms were based on Flory's [98] theory.

Recently, Izzo and Marques [99] studied theoretically, using scaling concepts, the formation of dilute phases of spherical, cylindrical, and planar aggregates of diblock A–B and triblock A–B–A copolymer chains in solvents selective to B. They treated the micelle formation of the triblock copolymers in the same way as that of the diblocks, the only difference being that the core was composed of twice as many chains of half the length of B. This resulted in $\Delta G^\circ_{\text{triblock}} \approx 2\Delta G^\circ_{\text{diblock}}$, which is counterintuitive and opposite to the micellization theories examined above. It thus appears that the entropy loss associated with the formation of loops is essential for describing the micellization of triblock copolymers. The loop (backfolding) entropy term was first introduced by ten Brinke and Hadziioannou [100] in their model of B–A–B copolymer micelle formation in A–homopolymer, and modified by Balsara et al. [101] in a similar model. Balsara et al. [101] commented on the applicability of the theory of Leibler et al. [88], originally proposed for micellization of A–B block copolymer in A–homopolymer, in the theories of Munch and Gast [90] and Nagarajan and Ganesh [91], that treat micellization in selective solvents. They noted that, in the presence of solvents, the description of the core–corona interface is complicated owing to the three-component (owing to the presence of solvent at the interface) nature of the problem [101]. These points, in addition to the hydrogen bonding interactions between both PEO and PPO, and water, may account for the quantitative discrepancy between predictions of phenomenological block copolymer micellization theories and the experimental results of Ref. [28] for the system PEO–PPO–PEO/water.

6.2. *Mean-field lattice models*

Another approach to modeling block copolymer micelles has used the Scheutjens–Fleer theory [102], an extension of the Flory–Huggins analysis of homogeneous polymer solutions [98], in which the polymer chains are allowed to assume different conformations on a lattice. A first-order Markov approximation (i.e. the position of a segment depends only on that of the preceding segment in the chain) is used in the Flory–Huggins analysis

and, as a result, the chain conformation follows the path of a random walk. In addition, a mean-field assumption is invoked to describe the interactions between different polymer segments. The free energy of the system is minimized in order to calculate the equilibrium thermodynamic properties of the polymer solution. For spatially inhomogeneous systems such as those containing interfaces, Scheutjens and co-workers [95,102,103] restricted the mean-field approximation to two dimensions (i.e. within parallel or concentric lattice layers) and applied a step-weighted random walk to account for the inhomogeneities normal to the layers. The polymer and solvent molecules are assumed to be distributed over a lattice, such that solvent molecules and polymer segments occupy one lattice site each. Each polymer chain can assume a large number of possible conformations, defined by the layer numbers in which successive segments are found. There can be many different arrangements for each conformation; if the number of polymer chains in each conformation is specified, the configurational entropy contribution to the system free energy can be evaluated. The other contributions to this free energy, due to the interactions between the polymer molecules, solvent molecules and the surface, are characterized by Flory–Huggins χ-parameters. If the free energy of the system is minimized with respect to the number of polymer chains in each conformation, it is possible to calculate the equilibrium segment density profiles. Self-consistent field theory can be used to calculate the segment density profiles in a micelle once the aggregation number of the micelle is known [95,103,104]. To find this aggregation number, small system thermodynamics can be used [105–107], according to which the change in free energy due to the change in the number of micelles (at constant temperature, pressure and number of molecules) must be zero at equilibrium. This "excess free energy" is the sum of the energy required to create micelles and the energy due to the translational entropy of the micelles. Since the segment density profiles are required in order to calculate the energy of micelle formation, an iterative process is followed. The self-consistent mean-field lattice theory of Scheutjens and Fleer [102] has been used to study many colloidal systems, including adsorption of homopolymers and block copolymers on surfaces [108], interactions between adsorbed polymer layers [109], and the formation of micelles [103], vesicles [104] and membranes [110].

Recently, the Scheutjens and Fleer theory has been extended by Hurter et al. [48,49] to study the formation of micelles by linear PEO–PPO–PEO and branched, star-like, amphiphilic block copolymers; the solubilization of naphthalene in these micelles has also been analyzed as a function of polymer structure, composition and molecular weight [48,49]. The detailed density profiles of the polymer segment in the micelles were obtained, and macroscopic quantities such as critical micellization concentration, aggregation number, and micelle size were calculated. The calculations show that higher-molecular-weight polymers form larger micelles. The addition of the solute causes the micelle to become larger, with a lower concentration of water and a higher concentration of PPO in the micelle core. The simple lattice theory for flexible chain molecules, however, cannot capture effects such as the phase behavior of PEO and PPO in water, where a lower critical solution temperature is observed. To predict such behavior, the gauche and trans bond orientations of the polymer chain must be accounted for. Leermakers [111] combined the rotational isomeric state scheme (which accounts for the gauche–trans orientations in a chain and eliminates back-folding) with self-consistent field theory to predict the formation of lipid bilayer membranes and lipid vesicles. An approach which is computationally more simple than the rotational isomeric state scheme, but nevertheless accounts for the temperature and composition dependence of the interaction parameter χ in a physically acceptable manner, has recently been presented by Karlstrom [46]. This model for PEO recognized that certain sequences of the gauche–trans orientations in an EO segment would lead to a polar conformation, while others would be essentially non-polar; the probability of non-polar conformations increased with temperature, making the polymer more hydrophobic. The solubility gap in PEO–water and PPO–water phase diagrams could be reproduced using this model.

A model for block copolymer micelles has been developed [48,50] which incorporates Karlstrom's ideas to account for the conformational distribution in PEO and PPO. An increase in temperature caused the model-predicted micelle aggregation number to increase, and the CMC concentration to decrease. The aggregation number increased rapidly with polymer concentration under dilute conditions, but was approximately invariant to polymer concentration at concentrations far from the CMC. Raising the PPO content or the molecular weight of the copolymer increased the aggregation number, and decreased the CMC. The model predicts that the most hydrophobic polymer, Pluronic P103, does not form spherical micelles at higher polymer concentrations, owing to phase separation or formation of aggregates of non-spherical structure. Fig. 15(a) shows the effect of PEO block size on the segment density profile and micelle size for PEO–PPO–PEO copolymers with the same PPO block [48]. An increase in PEO block size resulted in a smaller micelle core, while the corona became more extended. This is reflected in the decreasing aggregation number for the micelles shown in Fig. 15(b). The conformation of the polymer was affected by both the temperature and the composition of the surrounding solution; both PEO and PPO had a lower fraction of polar segments in the core of the micelles, and the polar fraction decreased with an increase in temperature. The micelle aggregation number was found to increase with an increase in the solute bulk concentration. This is in agreement with the experimental results of Al-Saden et al. [29], who found that the increase in the hydrodynamic radius of L64 aggregates upon hexane solubilization was greater than could be explained by the additional volume of the solute. It was postulated that the increase in hydrodynamic radius resulted from a combination of an increase in the aggregation number and the incorporation of the solute (hexane in the study of Ref. [29]).

The phase behavior of aqueous solutions of block polymers containing PEO and PPO has been modeled by Linse [51] on the basis of a mean-field lattice theory (similar to that used by Hurter et al. [48]) developed for multicomponent mixtures of copolymers with internal states occur-

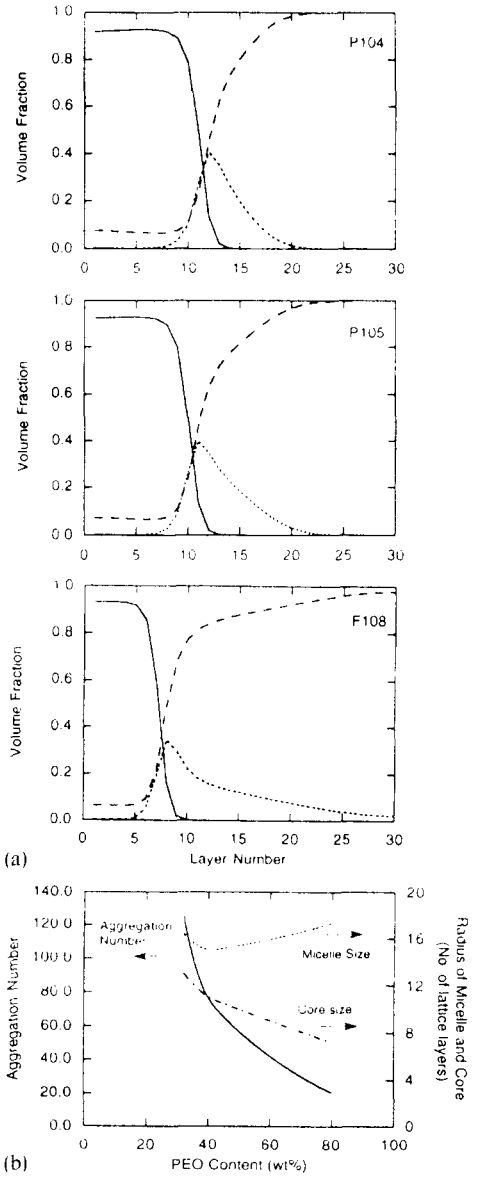

Fig. 15. (a) Effect of PEO block size on the segment density profiles in micelles formed by PEO–PPO–PEO copolymers having the same PPO block, as predicted by a self-consistent mean-field model. The volume fraction of PEO in the micelle is represented by the dotted lines, the volume fraction of PPO by the solid lines, and the volume fraction of water by the broken lines. An increase in PEO block size results in a smaller micelle core, while the corona becomes more extended. This is reflected in the decreasing aggregation number for the miceles as shown in (b). (Reprinted with permission from Ref. [49]; copyright American Chemical Society, 1993.)

ring in heterogeneous systems. The regions for unimer solution, spherical micelles, and elongated rods have been examined for three PEO–PPO–PEO triblock copolymers. A semiquantitative description of the strong temperature dependence of the phase behavior was obtained. At low polymer concentrations and temperatures a unimer solution was found, whereas at either higher temperatures or higher concentrations a solution of spherical micelles was present. A transition from spherical to infinitely long rod-like aggregates occurred at even higher temperatures, and eventually the system separated into two phases. Fig. 16 shows the phase diagram of Pluronics P105, P95, and P104 as predicted by the model of Linse [51]. A comparison of the phase diagrams indicated that a reduction of the copolymer molecular weight by approximately 20% at constant PPO/PEO composition ratio (i.e. from P105 to P95) led to an increase in CMC for a given temperature, a smaller micellar region, and a region of rods of a similar range but slightly shifted to lower temperatures. Decreasing the PEO block size, while keeping the PPO block constant (i.e. from P105 to P104), resulted in a shift of the CMC curve to lower copolymer concentration at a given temperature, a smaller micellar region, and a smaller region of rod-like aggregates which is shifted considerably to lower temperatures [51]. Comparison of the modeling predictions for the phase diagram of Linse [51] with the experimentally determined phase diagram of Mortensen [61] reveals qualitative agreement with respect to the number of phases occurring and their relative location. However, the calculated CMC curve occurred at temperatures 20–30 K higher than those experimentally observed, and the calculated region for the hexagonal phase occurred at a lower temperature, thus leading to a temperature range for the micellar solution phase which is too narrow. Segment density profiles indicated that, at a given concentration, the radial extension increased whereas the headgroup area decreased with increasing temperature for both micelles and rods. At the transition from micelles to rods the radial extension was reduced abruptly by approximately 10% [51].

In addition to phase behavior, Linse [50] used

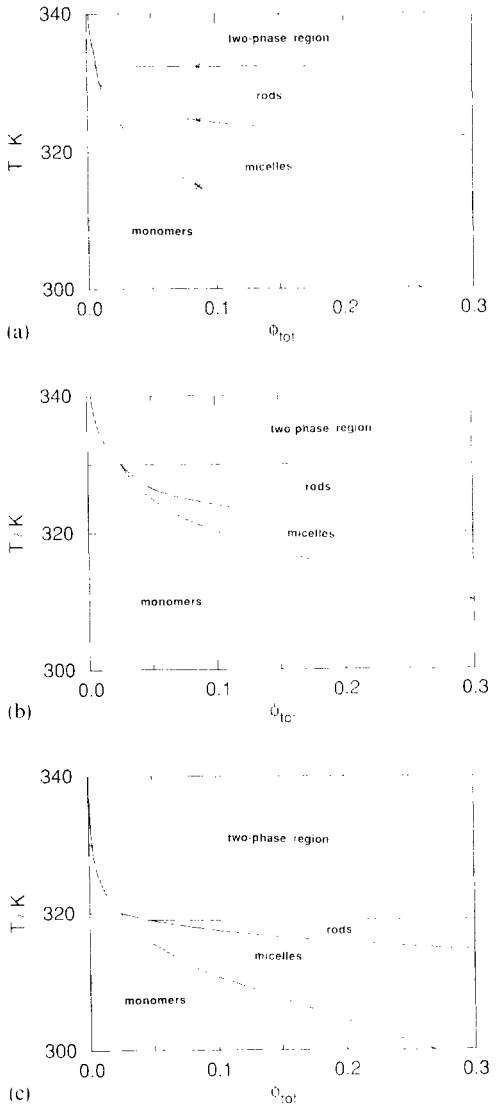

Fig. 16. Phase diagrams of (a) P105, (b) P95, and (c) P104 Pluronic PEO PPO–PEO copolymers (predicted by a self-consistent mean-field model model) indicating regions of unimers, micelles, rods, and phase separation. (Reprinted with permission from Ref. [51]; copyright American Chemical Society, 1993.)

the model to predict micellization properties (i.e. CMC, aggregation number, hydrodynamic radius) and their temperature dependence for Pluronic copolymer solutions. Fig. 17(a) shows the CMC and the concentration of the free polymer as a function of temperature for various PEO–PPO–PEO

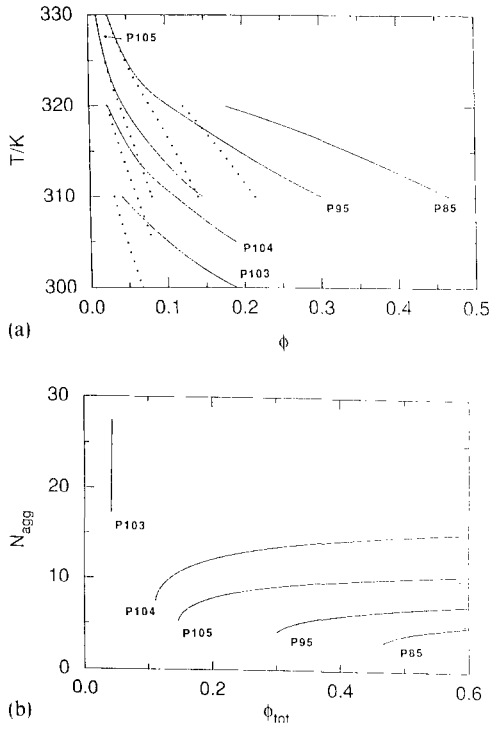

Fig. 17. (a) Calculated (by a self-consistent mean-field model model) CMC (—) and the concentration of free polymer (···) as a function of temperature for Pluronics P85, P95, P105, P104, and P103. (b) Effect of varying the copolymer PEO/PPO composition (at a given temperature) on the micellar aggregation number. (Reprinted with permission from Ref. [50]; copyright American Chemical Society, 1993.)

copolymers [50]. Both the PPO/PEO ratio and the copolymer molecular weight influence micellization, in qualitative agreement with experimental CMC data [28]. The effect of varying the copolymer PPO/PEO composition (at a given temperature) on the micellar aggregation number is presented in Fig. 17(b) [50]. For PEO–PPO–PEO polymers with the same PPO/PEO composition, increasing the molecular weight resulted in increasing the aggregation number. Note also that the model predicted an "infinite" aggregation number for Pluronic P103, similar to the predictions of Hurter et al. [48,49].

The self-consistent mean-field theory used by Hurter et al. [48,49] and Linse [50,51] was able to reproduce the anomalous phase behavior of PEO and PPO homopolymers, predict the micellization behavior of PEO–PPO–PEO block copolymers, and provide detailed information on the microstructure of the micelles. Copolymers of varying blockiness and block sequence could be handled, and no a priori assumptions with respect to the core–corona interface were necessary. The model calculations showed qualitative agreement with experimental predictions on the effect of temperature, concentration, hydrophobicity, and molecular weight of the polymer; quantitative agreement was also good, considering that all the model input parameters were obtained from independent experiments. The phenomenological theory of Nagarajan and Ganesh [91], developed originally for diblock copolymers and extended to triblocks by Prochazka et al. [97], was also successful in predicting qualitatively the contributions of copolymer composition and molecular weight to the micellization of triblock PEO–PPO–PEO copolymers (although the predicted CMCs were unreasonably low). A sharp interface had to be assumed, however, between the core and the corona, and variation of the number of blocks or block sequence was not straightforward. Further, the effects of temperature on micellization were not examined. An advantage of the Nagarajan and Ganesh theory is that the various contributions to the micellization free energy were easily quantified, leading to a better appreciation of their magnitude and influence on the micellization.

7. Surface activity of PEO–PPO copolymers

7.1. Adsorption at the air–water interface

Surface tension data for various Pluronic PEO–PPO–PEO copolymer aqueous solutions have been reported by Alexandridis et al. [112] at two temperatures, 25 and 35°C. Fig. 18 shows surface tension values for Pluronics P105 and P85, plotted semilogarithmically with respect to the copolymer concentration in the solution [112]. At low concentrations the surface tension decreased with increasing concentration for all copolymers, in accordance with the Gibbs adsorption isotherm [113]. A change in slope (break) was observed in the surface tension curve at a characteristic concentration, after which the surface tension values

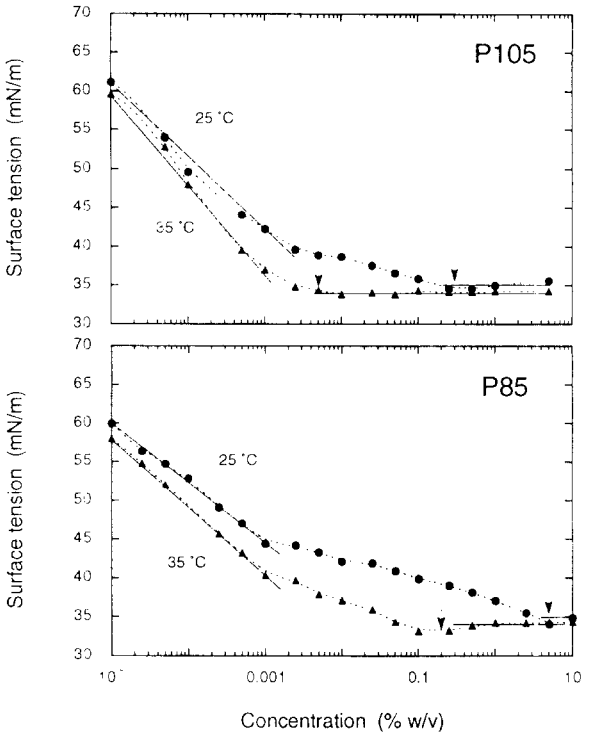

Fig. 18. Surface tension for Pluronic P105 and P85 aqueous solutions, plotted as a function of copolymer concentration at 25 and 35 °C. (Adapted with permission from Ref. [112]; copyright American Chemical Society, 1994.)

continued to decrease until a plateau was reached (second break); the surface tension values remained constant with further increase in copolymer concentration [112]. This behavior (two breaks) was observed for most copolymers studied and was very reproducible. The first (low-concentration) break occurred at a copolymer concentration of approximately 0.001%, which was roughly the same for both temperatures studied and for a number of copolymers. The surface tension value at the onset of this break varied from 40 to 50 mN m^{-1}. The presence of two breaks has led to some confusion in the literature on PEO–PPO–PEO copolymers regarding the interpretation of the surface tension dependence on concentration, and the extraction of the CMC from such a set of data [30,114,115]. In most cases it has been assumed that the first change in slope signified the CMC [115,116], although other interpretations, such as formation of "unimolecular" micelles [114], have been given. The region of decreasing surface tension that follows the break at 0.001%, and the second break have often been ignored [114,115], but it has been suggested that they were due to broad copolymer molecular weight distribution and to the presence of impurities [30].

Good agreement between the CMCs determined from dye solubilization [28] and the concentration at the second break of the surface tension curve has been shown [112], leading to the conclusion that the higher-concentration break corresponds to the CMC and signifies the formation of polymolecular micelles with a well-defined hydrophobic interior (i.e. able to solubilize organic solutes). It should be noted that the copolymer concentrations at the second break, extracted from the surface tension data of Wanka et al. [30] (0.3% for F127, and 0.01% for P104, both at 25 °C) and Prasad et al. [114], are also comparable with the CMC values found in the dye solubilization study of Alexandridis et al. [28]. Two other observations supporting the conclusion that the higher-concentration break is the CMC are (i) the plateau observed in the surface tension values after the high-concentration break, and (ii) the effect of temperature on the copolymer concentration at which the second break occurs. Attainment of a constant surface tension value is an indication of micelle formation (CMC) in solutions of typical surfactants [113]. While the surface tension of Pluronic copolymer solutions keeps decreasing with increasing copolymer concentration after the first low-concentration break, it remains constant after the second break (a dip in the surface tension after the break observed for Pluronic P85 is most likely due to impurities [26,40,117]). Regarding the effect of temperature, the copolymer concentration at which the second change in slope occurs decreased significantly with increasing temperature, in good agreement with the CMCs obtained from dye solubilization [28] and observations in other studies of Pluronic copolymers [27,64], whereas the concentration at the first break did not vary significantly [112].

Having attributed the high-concentration break (change in the slope) of the surface tension curve to the formation of micelles in the bulk (CMC), we examine the region below the origin of the first

(low-concentration) break. The wide molecular weight distribution of the copolymers studied, and the presence of hydrophobic impurities, have been singled out in the past as possible factors causing differences in the CMC values obtained by surface tension and dye solubilization methods. The effect of molecular weight distribution on the surface tension of non-ionic surfactants has been nicely demonstrated by Crook et al. [118], who studied the surface tension of normal (Poisson) distribution and single species octylphenoxy–ethoxyethanols (OPE_{1-10}, where 1–10 is the number of ethylene oxide segments), and mixtures of single species and normal distribution OPE_4 and OPE_{10}. The authors found preferential adsorption of molecules of shorter PEO-chain length (OPE_{3-5}) at the air–water interface; this was demonstrated by a less sharp (but still, only single) break in the surface tension curve, and a dip in the surface tension values in the vicinity of the break. Such behavior was attributed to the replacement of highly surface active, short PEO-chain-length molecules (contributing to a low surface tension value) on the interface by the major component, when these highly surface active molecules were solubilized in micelles formed by the major component. No manifestations of the above were seen in the surface tension curves for Pluronics [112]. As for the influence of impurities, a decrease in surface tension with time, observed in some experiments at low copolymer concentrations, would indicate the presence of hydrophobic impurities that adsorb slowly on the surface [117]. However, the presence of such impurities should result in a lowering of the surface tension (described above as a "dip") below the steady value obtained after the CMC. Such a "dip" was not observed in the vicinity of the low-concentration break in the surface tension curve, but can be seen in some of our experiments (e.g. Pluronic P85) at the high-concentration break. It can thus be concluded that neither polydispersity of the copolymer size nor hydrophobic impurities cause the low-concentration break observed in the surface tension curves of PEO–PPO–PEO solutions.

It has been proposed that the low-concentration break in the surface tension vs. copolymer concentration curves is due to a change in configuration (structural transition) of the copolymer molecules at the air–water interface [112]. Constant surface coverage has been attained at bulk copolymer concentrations ranging from 10^{-6} to 10^{-3}%, with the PEO–PPO–PEO copolymer molecules adsorbed at the interface possibly as an inverted "U" (this is one of the proposed orientations for homopolymer PEO at the interface [119]) and the PEO chains located at the air–water interface. At a bulk concentration of approximately 10^{-3}%, a structural transition occurs and the copolymer layer becomes more compact; water is expelled [120] and PEO segments protrude into the aqueous solution [121] or fold around PPO. More copolymer molecules can fit at the interface (causing it to become thicker [122]) and the surface tension continues to decrease with increasing bulk copolymer concentration, but at a slower rate (note also that a bulk concentration of 10^{-3}% is comparable to the bulk PEO concentration required for full coverage of the air–water interface according to Glass [123] and the bulk PPO concentration at which phase separation occurs [124]). On formation of micelles in the bulk, a further increase in the number of copolymer molecules in the bulk is accommodated by an increase in the number of micelles, the activity of the copolymer in the bulk remains approximately constant, and the surface tension attains a steady value that does not change with further increase in the bulk copolymer concentration.

The values for surface area per copolymer molecule, calculated through the Gibbs adsorption isotherm [112,114], are generally small compared to those of non-ionic surfactants with an aliphatic chain and PEO headgroup (of comparable size to the PEO block of Pluronics) [125,126], indicating that there is considerable folding of the polymers at the air–water interface [114] and/or desorption of PEO segments in the water phase [127,128]. The area per copolymer molecule increased with the number of EO segments in the molecule for a family of Pluronic copolymers with the same PPO and varying PEO block length, as seen in Fig. 19 [112]. Also shown on the same plot are areas per molecule for a series of octylphenoxy–ethoxyethanol surfactants (area values were extracted from Crook et al. [118]). An increase in the length of

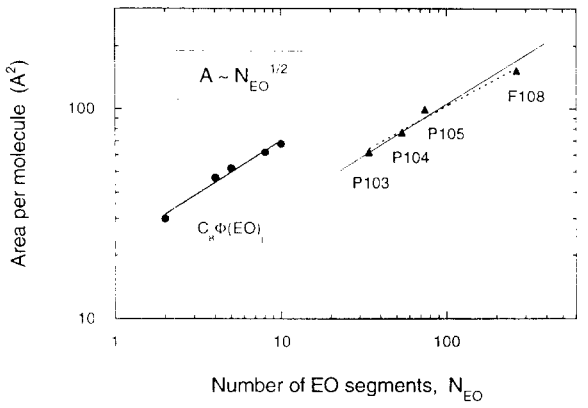

Fig. 19. Area per PEO–PPO–PEO copolymer molecule plotted as a function of the number of EO segments. Also shown on the same plot are areas per molecule for a series of octylphenoxy–ethoxyethanol surfactants (area values were extracted from Ref. [118]). (Reprinted with permission from Ref. [112]; copyright American Chemical Society, 1994.)

the hydrophobic (PPO) block, for a group of copolymers that have the same PEO block size, resulted in a decrease in the area that each molecule occupies at the air–water interface, in agreement with Prasad et al. [114]. This finding suggests a more compact interfacial layer for larger PPO segment size, with the copolymer molecules oriented on the surface in a coiled manner having PPO out of the aqueous phase, and the hydrophilic PEO segments at the extremities of the copolymer partly anchoring the polymer in the aqueous phase and partly folding around PPO.

The areas per molecule reported by Yeates et al. [129] were higher for $C_1E_8C_i$ than for $C_iE_{15}C_i$ (C = methyl group, $i = 5$–12, E = ethylene oxide group), indicating again that the hydrophobic moiety makes the interfacial layer more compact. Phipps et al. [121] studied the conformation of Pluronic F127 at the hexane–water interface employing a neutron reflectivity technique. Use of hexane was necessary to achieve contrast variation; however, the authors report indications that the presence of hexane had little effect on either the adsorbed amount or the conformation of the copolymer on the water side of the interface; in this respect, their findings should also be applicable to copolymers adsorbed at air–water interfaces. Pluronic F127 was found to adopt a conformation that extended beyond the micellar radius in water and, thus, appeared quite stretched. The estimated (unperturbed) radius of gyration of a PEO block is 2.0 nm and that of the PPO block 1.6 nm; the volume fraction profile of F127 at the interface (fitted from the neutron scattering data) showed the PEO segments to protrude 9 nm into the water subphase and PPO to extend 4 nm into hexane [121]. On the contrary, a random copolymer of poly(vinyl alcohol-*co*-acetate) was found to adopt a very flat conformation at the interface, forming a dense layer of approximately 2 nm thickness. The experimental findings regarding the conformation of the Pluronic copolymer at the interface were borne out by a Scheutjens–Fleer simulation (similar to the one used for modeling block copolymer micelles [48–51]) that showed the copolymer attached to the interface by the hydrophobic PPO block and the PEO blocks having a "parabolic" segment density profile, similar to a polymer chain grafted at a solid surface. Both the protrusion of PEO in the water subphase and the resemblance of PEO to a grafted chain agree with the findings of the surface tension study of Alexandridis et al. [112].

7.2. *Adsorption at solid–water interfaces*

The adsorption of several Pluronic PEO–PPO–PEO copolymers (L61, L62, L64, F38, F68, F88, and F108) onto polystyrene latex particles was described by Kayes and Rawlins [130]. Langmurian isotherms were obtained and, in general, maximum adsorption occurred after the measured apparent CMC. The areas occupied by a copolymer molecule at the interface in the plateau region of the adsorption isotherm were found to be greater than those observed at the air–water interface [112,114], and considerably less than those at a quartz–water interface (reported in an early study by Heydegger and Duning [131]), indicating the importance of the nature of the interface on adsorption. The area-per-molecule values measured were 2.85, 3.20, 5.90, 6.51, 15.10, 17.52, and 24.26 nm^2 for Pluronics L61, L62, L64, F38, F68, F88, and F108, respectively. Examination of the molecular areas at the interface showed that the adsorbed PPO blocks formed small loops or

were tightly coiled on the surface; this was confirmed by determination of the adsorbed layer thickness from light scattering and electrophoresis experiments [130].

Baker and Berg [132] investigated the adsorption configuration of PEO and its copolymers with PPO (Pluronic triblock copolymers P75, P85, F68, F98, F108, and random PEO–PPO copolymers 50-HB-260, 50-HB-2000, 50-HB-5100) on model polystyrene latex dispersions. Adsorption isotherms and adsorbed layer thickness (determined from dynamic light scattering) for a number of Pluronics on latex particles are presented in Fig. 20 [132]. The adsorption isotherms exhibited the expected behavior, both adlayer thickness and specific adsorption increasing with the PEO block size and the bulk polymer concentration. The thickness isotherms have essentially the same shape as conventional high-affinity specific adsorption isotherms, rising rapidly at low concentrations and leveling off at bulk polymer concentrations corresponding to the plateau adsorption coverage. The specific adsorption values for Pluronics reach their plateau values at bulk copolymer concentrations slightly higher than the copolymer CMCs. In addition, the concentration corresponding to the adsorption plateau is well above the concentration required to create a monolayer of polymer segments at the particle surface (assuming all segments are in contact with the surface). These data suggest that the polymers adsorb in the extended configuration, with thin PPO loops and trains attached to the surface and longer PEO tails extending away from the surface [132]. Berg and co-workers [133] also studied the effect of particle radius on the hydrodynamic thickness of adsorbed PEO homopolymers and PEO–PPO–PEO copolymers. In the latter case, the adlayer thickness increased with particle radius, but the dependence was more complex than that of PEO adsorption.

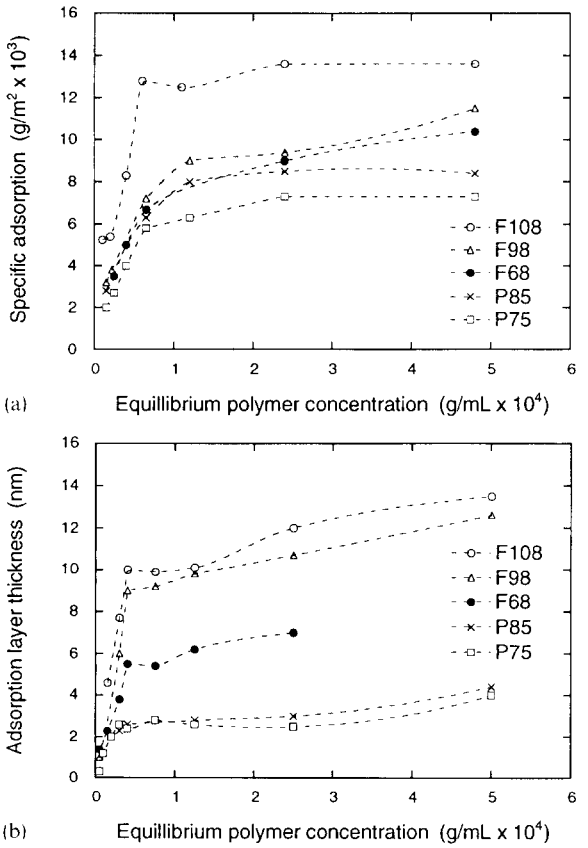

Fig. 20. (a) Adsorption isotherms and (b) adsorbed layer thickness (determined from dynamic light scattering) for a number of Pluronic copolymers on latex particles: □, P75; X, P85; ●, F68; △, F98; ○, F108. (Adapted with permission from Ref. [132]; copyright American Chemical Society, 1988.)

The effect of surface modification of polystyrene latex particles on subsequent protein adsorption was studied by Lee et al. [134]; the surface modifiers used were Pluronic PEO–PPO–PEO block copolymers. The hydrodynamic thickness δ_h of the adsorbed (on the particles) copolymers is plotted against the number of EO segments in Fig. 21 [134]. Shown for comparison as curves A and B are the dimensions for a rod-like chain and a coil-like chain. The scaling exponent of the fit to the experimental points suggested a coil-like chain conformation for the PEO blocks of the adsorbed copolymers. Fig. 21 shows that the dimensions of the adsorbed Pluronic copolymers are smaller than those of the extended rod-like chain (curve A), but larger than those of the adsorbed PEO homopolymer (curve B). Those δ_h values are also larger than the corresponding free surfactant unimer dimensions, suggesting that the picture of "loops and trains" for the hydrophobic PPO block and "loops and tails" for the hydrophilic PEO blocks is a suitable description for the adsorbed copoly-

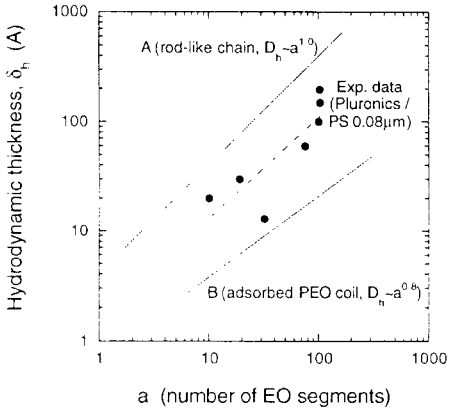

Fig. 21. Hydrodynamic thickness δ_h of adsorbed Pluronic PEO–PPO–PEO copolymers plotted against the number of EO segments. Curve A is the extended chain dimension according to $D_h = a$ (3.7 Å). Curve B represents δ_h vs. degree of polymerization for adsorbed PEO homopolymer. (Adapted with permission from Ref. [134]; copyright Academic Press, 1989.)

mers [134], in agreement with the study of Baker and Berg [132].

Killmann et al. [135] reported on the hydrodynamic layer thickness of PEO homopolymer and PEO–PPO–PEO copolymers adsorbed on polystyrene latex and precipitated silica particles. The conformation of the adsorbed polymer was determined by the surface–polymer interactions: hydrophobic interactions exist on the apolar latex surface, whereas hydrogen bonds dominate on the polar silica surface. PEO–PPO–PEO copolymers adhered to the latex via the hydrophobic PPO segments; the PEO blocks extended into the solution as tails, and the layer thickness depended on the molar mass of the PEO blocks. The adsorption mechanism of PEO–PPO–PEO copolymers on silica resembled that of PEO homopolymer; the adlayer thicknesses of the block copolymers were very small and comparable to the thickness of PEO adlayers on silica [135].

The adsorption of PEO–PPO–PEO block copolymers on silica, as well as the adsorption of PEO homopolymer, has been studied by Tiberg et al. [136] and Malmsten et al. [137]. For a number of polymers with a total molecular weight of approximately 15 000, it was found that the adsorbed amount is rather low (0.35–0.40 mg m^{-2}) and independent of the PPO content in the range 0–30% PPO. For a copolymer with a total molecular weight of 4000 and 50% PPO content, the adsorbed amount was approximately 0.20 mg m^{-2}. Thin adsorbed layers, with hydrodynamic thicknesses of approximately 2–5 nm, were formed by all polymers investigated. The pH dependence of the adsorbed amount and the hydrodynamic thickness were similar to that displayed by PEO homopolymers. Ellipsometry experiments provided information on both adsorption and desorption kinetics, both of which are fast processes in these systems and occur over a number of minutes. Finally, ellipsometry experiments showed that an abrupt increase in the adsorbed amount occurred prior to micelle formation in the solution. At temperatures above the CMT, the adsorbed amount remained independent of temperature (in the temperature range studied). The hydrodynamic thickness was much smaller than the hydrodynamic diameter of the solution micelles for all temperatures [137]. No abrupt increase in the adsorbed amount was observed on hydrophobic surfaces, although a strong increase in the adsorbed amount was observed as the system approached the phase boundary. The qualitative aspects of this finding were predicted theoretically as being a consequence of a partial phase separation phenomenon due to elevated copolymer concentration in the surface zone [136]. The experimental findings were interpreted using a modified mean-field theory which takes the reverse temperature phase behavior of the system into account [136,137].

8. Gels formed by PEO–PPO–PEO block copolymers

PEO–PPO–PEO copolymer solutions of high copolymer concentration exhibit a dramatic change in viscosity at temperatures close to ambient, revealing a "thermoreversible gelation" [27,30,40,138,139]. Several mechanisms have been proposed as driving forces for this thermal gelation: Rassing and Attwood [140] related the gel transition to intrinsic changes in the micellar properties. Vadnere et al. [141] discussed the gelation in terms of entropic changes involving locally ordered water

molecules close to the hydrophobic PPO segments, whereas Wanka et al. [30] and Wang and Johnston [138] speculated on the possibility of an ordered three-dimensional structured state or network. Recently, neutron scattering studies showed that the observed change in viscosity is due to a "hard-sphere crystallization" as the micelle concentration approaches the critical volume fraction of 0.53 (micelles close-packed) [61,64]. At even higher temperatures the gel "dissolves" again. The PEO chains in the micellar mantle interpenetrate extensively in the gel, yielding a dynamic correlation length of magnitude 0.8 nm at the highest concentration used (about 0.35 g ml^{-1}) [57]. Oscillatory shear measurements show that the gelation onset temperature and the thermal stability range of the gel increase with increasing PEO block length [57].

Ultrasonic relaxation and ^{13}C NMR spectra were reported for Pluronic F127 dissolved in water and D_2O, respectively, by Rassing et al. [142]. The polymer solution exhibited reverse thermal behavior; a 20% w/w solution formed a gel at room temperature. The ultrasonic relaxation, as well as the methyl carbon resonance, of the PPO block showed distinct anomalies over the temperature range in which the gel formation takes place. Such anomalies, however, were also observed in dilute solutions where a gel is not being formed. It was deduced, on the basis of the results obtained, that observed relaxations arose predominantly from conformational changes related to alternations in the orientation of the methyl group side chains in the PPO block of the polymer. These conformational changes were thought to be induced by extrusion of hydrated water with increasing temperature from the existing micelles, the interiors of which consist of the PPO segments. It was further proposed that the dehydration, which causes a higher friction between the end groups in the polymer chain, was responsible for the reverse thermal behavior of the viscosity and, hence, for the gel formation in concentrated copolymer solutions [142].

The temperature-induced gelation in Pluronic F127 copolymer solutions was reflected in the rapid increase of the storage modulus by two or more orders of magnitude [30]. The storage modulus G' approached a steady value after gel formation, which increased with increasing copolymer concentration [30]. The gel formation temperature decreased with increasing polymer concentration. The copolymer gels exhibited a characteristic yield stress at which they flow when stress is applied. The yield value was zero for solutions below the gel temperature, and increased above the gel temperature with further increase in the temperature. The yield value increased with polymer concentration; the highest yield values were above 1000 Pa. Wanka et al. [30] also note that the gels were not birefringent, indicating that they were not anisotropic liquid crystalline phases. Brown and co-workers [27,57] measured the viscoelastic properties of Pluronics P85, P87, and F88 as a function of temperature. They defined the gelation temperature as the temperature at which storage molulus, G', equals the loss shear modulus, G''. The gelation temperature for Pluronic P85 is presented as a function of concentration in Fig. 22(a) [27]. P85, P87, and F88 showed qualitatively similar gelling behavior, but with important quantitative differences as shown in Fig. 22(b) [57]. P85 formed a gel at 35°C at 20% copolymer concentration. It can also be seen in Fig. 22(b) that P85 formed a gel over a rather narrow temperature interval (up to 48°C), whereas P87 and F88 remained as gels up to 80°C. The maximum values of G' are similar for F87 and F88, and somewhat smaller for P85. Brown et al. [57] concluded that the gelation onset temperature and the thermal stability range of the gel increased with increasing PEO block length.

The sol–gel transition temperature was measured as a function of copolymer concentration for nine Pluronic PEO–PPO–PEO copolymers by Vadnere et al. [141]. Fig. 23(a) shows a plot of the logarithm of the copolymer concentration vs. $1/T$ for some of the polymers studied in Ref. [141]. The enthalpy of gelation, ΔH°_{gel}, was estimated from a relationship similar to that used for obtaining ΔH° of micellization from CMC vs. temperature data (see Section 4.1). A positive enthalpy change between 5 and 10 kcal $mol.^{-1}$ of copolymer was observed in all cases. Unlike the gelation of gelatine, where the large enthalpy change (-67 kcal mol^{-1}) favors the gelation process, the

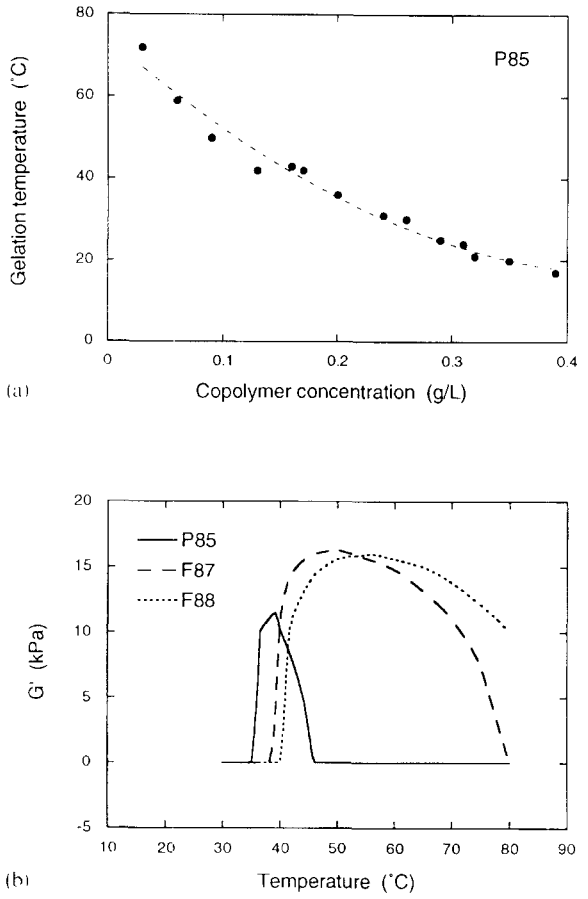

Fig. 22. (a) Gelation temperature (determined from oscillatory shear measurements) as a function of Pluronic P85 concentration (adapted with permission from Ref. [27]; copyright American Chemical Society, 1991.) (b) Comparison of temperature-dependent gelation of 0.25 g ml^{-1} solutions of Pluronics P85, P87, and F88. (Adapted with permission from Ref. [57]; copyright American Chemical Society, 1992.)

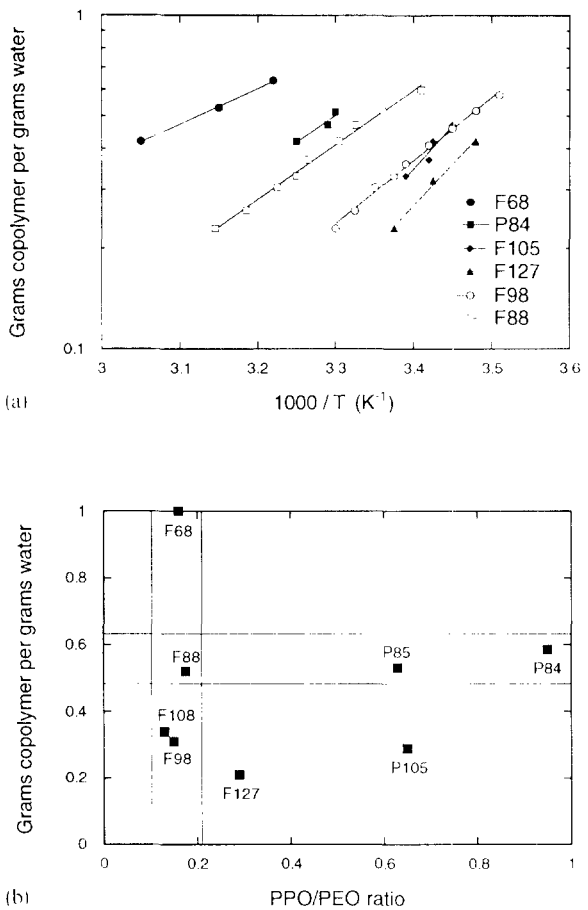

Fig. 23. (a) Logarithm of copolymer concentration vs. inverse gelation temperature for various Pluronic PEO PPO PEO copolymers. (b) Concentration of copolymer required to give a gel transition temperature of 25 °C, plotted as a function of the copolymer PPO/PEO composition ratio. (Adapted from Ref. [141].)

enthalpy change in the case of PEO–PPO–PEO gelation is unfavorable. The copolymer concentration required to give a gel transition temperature of 25 °C is plotted in Fig. 23(b) as a function of the PPO/PEO composition ratio [141]. The following trends were noted: the concentration required for gel formation was approximately the same for copolymers with the same size PPO block; for a given PPO/PEO ratio, the polymer concentration required for formation of a gel (at a given temperature) decreased with increasing molecular weight; in fact, a linear relationship was observed between log M_w and $1/T$ for copolymers with the same PPO/PEO ratio. The presence of NaCl, KCl, and $NaSO_4$ decreased the gel transition temperature, whereas the opposite effect was observed with urea, alcohol and sodium dodecylsulfate. The enthalpy of gel formation was not significantly altered by the added substances, suggesting that entropy plays the major role in the gelation process [141].

The potential of using Pluronic F127 gels for controlled drug delivery was studied by Gilbert et al. [143]; the effect of solutes and polymers on the gelation properties was also reported. The

gelation temperature was determined for a range of F127 concentrations (24–34%) with benzoic acid loading increasing from 0 to 2% w/v. The gel–sol transition temperature decreased as the benzoic acid concentration increased [143]. The homologous series of *para*-hydroxybenzoate esters, methyl, ethyl, propyl, and butyl, were also considered: the more lipophilic compounds resulted in a greater decrease in the gel–sol temperature for all copolymer concentrations studied. Addition of PEO homopolymer increased the gelation temperature; the extent of this increase depended on the added PEO chain length and concentration. The effect of additives on gel formation in aqueous F127 solutions has also been reported by Malmsten and Lindman [59,60,144]. The stability range of the gel phase depended strongly on the presence of salts. NaCl, which is often referred to as a typical "salting out" cosolute, displaces the whole gel region, as well as the cloud point, to lower temperatures, as shown in Fig. 24 [59]. NaSCN, a typical "salting in" cosolute, displaces the whole gel region and the cloud point up to higher temperatures (see Fig. 25) [59]. The effects of added PEO and PPO homopolymers were also investigated. It was found that PEO of intermediate molecular weight caused the gel to "melt" at a certain homopolymer amount which depended on the copolymer concentration. The efficiency of PEO in inducing melting of the gel increased with PEO molecular weight, but at very high PEO molecular weights phase separation (rather than gel melting) occurred. The gel melting behavior was also observed upon addition of a cationic polyelectrolyte, poly(diallyldimethylammonium chloride) (PDADMAC). Addition of PPO homopolymer, however, tended to increase the stability region of the gel, although this depended on the PPO molecular weight [144].

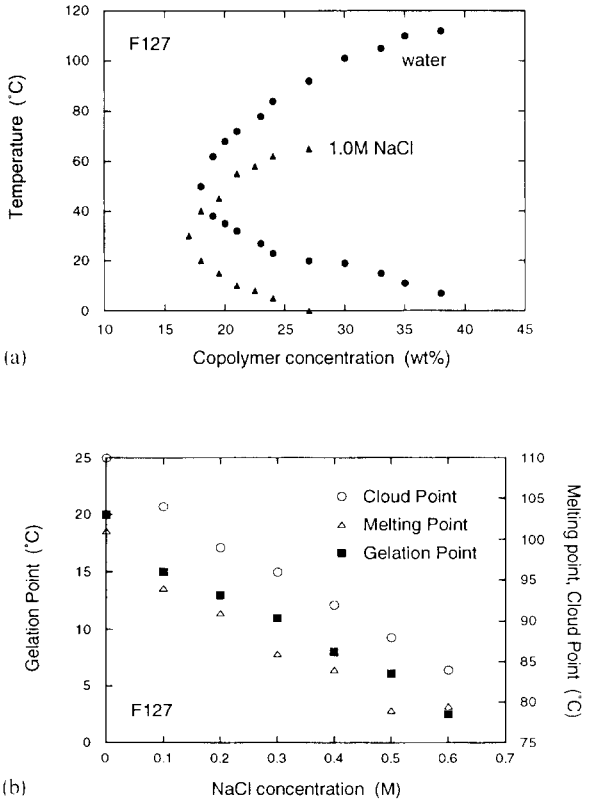

Fig. 24. (a) Phase behavior of the F127/water system in the presence of 1.0 M NaCl. Also shown is the phase diagram for the polymer/water system. (b) Gelation point (GP), melting point (MP), and cloud point (CP) of a 30% F127 solution as a function of NaCl concentration. (Adapted with permission from Ref. [59]; copyright American Chemical Society, 1992.)

9. Comparison of PEO–PPO copolymers with other non-ionic copolymers and surfactants

9.1. PEO–PBO block copolymers

A significant amount of information on the synthesis and solution behavior of block copolymers composed of PEO and poly(butylene oxide) (PBO) has been reported in the last few years by the groups of Attwood, Price, and Booth from the University of Manchester. According to them PEO–PBO–PEO copolymers have the advantage of greater composition and chain length uniformity over comparable PEO–PPO–PEO copolymers. Luo et al. [145] note that the preparation of PEO–PPO–PEO copolymers involves the anionic polymerization of propylene oxide (PO) to form difunctional PPO, followed by polymerization of ethylene oxide to form the outer blocks; the anionic polymerization of PO is complicated by a side reaction, involving hydrogen abstraction from the methyl group of PO to form allyl alcohol, which leads to initiation of additional monofunctional PPO chains and, in turn, to diblock copolymers

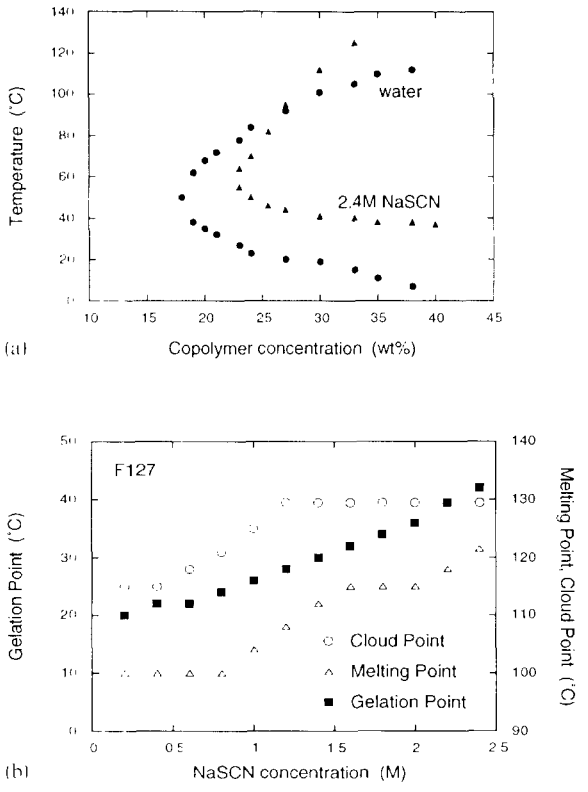

Fig. 25. (a) Phase behavior of the F127/water system in the presence of 2.4 M NaSCN. Also shown is the phase diagram for the polymer/water system. (b) Gelation point (GP), melting point (MP), and cloud point (CP) of a 30% F127 solution as a function of NaSCN concentration. (Adapted with permission from Ref. [59]; copyright American Chemical Society, 1992.)

with a different PPO content. The anionic polymerization of butylene oxide, however, is more straightforward, since transfer does not occur and difunctional PBO can be exclusively produced.

Luo et al. [145] prepared, using sequential anionic copolymerization, a poly(ethylene oxide)–poly(butylene oxide)–poly(ethylene oxide) triblock copolymer, denoted $EO_{58}BO_{17}EO_{58}$, where EO represents ethylene oxide and BO represents butylene oxide, and determined its micellar and gelation properties in aqueous solution. Surface tension, light scattering intensity, photon correlation spectroscopy, and gelation measurements were made at various temperatures over copolymer concentrations ranging from dilute solution to the gel (>20%). Surface tension measurements at 30 C over the 10^{-3}–10 g l^{-1} concentration range showed a single break at 0.3 g l^{-1}, indicative of the CMC. The CMC of the $EO_{58}BO_{17}EO_{58}$ copolymer was lower that the CMC of Pluronic F68, a PEO–PPO–PEO copolymer of comparable molecular weight and PEO composition. The micelle radius was approximately 6 nm, while the micelle "molecular" weight increased with temperature; the aggregation number was 13 at 30 C and 20 at 55 C. The micellization enthalpy, ΔH°, was estimated to be 34 kJ mol^{-1} from analyzing CMC vs. temperature data. The lower and upper temperature boundaries for the gel region were identified, and the occurrence of syneresis (separation of water from the gel) was noted. Nicholas et al. [146] compared the micellar and gelation properties of $EO_{58}BO_{17}EO_{58}$, $EO_{71}BO_{28}EO_{71}$, and $EO_{132}BO_{53}EO_{132}$ copolymers in aqueous solutions; the copolymers had similar PEO compositions (75–80 wt.% PEO) but different chain lengths (the copolymer molecular weights were 7000, 8800, and 17 500, respectively). Measurements were made at 30 C over a wide concentration range. Critical micellization and gel concentrations decreased markedly as the copolymer chain length increased, while micellar weights and sizes increased. The CMCs for $EO_{71}BO_{28}EO_{71}$ and $EO_{132}BO_{53}EO_{132}$ were 0.16 and <0.02 g l^{-1}, respectively; the aggregation numbers were 40 and 600 for $EO_{71}BO_{28}EO_{71}$ and $EO_{132}BO_{53}EO_{132}$, respectively. Phase separation was observed in dilute solutions of the copolymer of higher molecular weight ($EO_{132}BO_{53}EO_{132}$). The micellar, gelation and drug release properties of aqueous $EO_{40}BO_{15}EO_{40}$ solutions were investigated by Luo et al. [147]. A brief investigation of the rate of release of salicylic acid from the gel served to illustrate useful sustained release. The gelation behavior, interpreted via the hard-sphere model, was consistent with the measured micellar sizes.

Diblock PEO–PBO copolymers have also been synthesized and characterized by the Manchester group. Sun et al. [148] reported preliminary results on the preparation of $EO_{135}BO_{33}$ and its micellization and surface properties in dilute aqueous solutions. Six PEO–PBO diblock copolymers ($EO_{92}BO_{7}$, $EO_{50}BO_{13}$, $EO_{40}BO_{8}$, $EO_{50}BO_{4}$, $EO_{24}BO_{10}$, and $EO_{27}BO_{5}$) have been prepared by Beddels et al. [149], and their micellization in

aqueous solution investigated. Surface tension, static and dynamic light scattering and gel permeation chromatography techniques were used to study solutions at temperatures in the range 20–50°C over a wide concentration range (up to 100 g l^{-1}). CMCs, micellar molar masses and radii have also been reported [149]. The thermodynamics of micellization of EO_mBO_n diblock copolymers was discussed in relation to that of related triblock copolymers ($EO_mBO_nEO_m$ and $EO_mPO_nEO_m$). Tanodekaew et al. [150] prepared a series of diblock copolymers $EO_{30}BO_n$ (with n in the range 3–16) by sequential anionic polymerization, and investigated the association behavior of the copolymers in aqueous solution and the gelation of their concentrated micellar solutions. At temperatures in the range 30–50°C, a minimum PBO block length of 4 to 5 units was required for micellization. Gelation of micellar solutions of the copolymers was observed for copolymers with PBO block lengths of 6 to 7 units or more. The relationships between (i) standard Gibbs energy of micellization and molecular characteristics and (ii) critical gelation concentration and micellar characteristics were explored. Diblock PEO–PBO copolymers (allyl-$BO_{12}EO_{15}$, allyl-$BO_{12}EO_{25}$, and allyl-$BO_{12}EO_{35}$) were investigated by Hatton and co-workers [151]. The formation of micelles was studied using fluorescence methods and the thermodynamic parameters of micellization estimated from a closed association model; the micelle hydrodynamic radii (R_h) were also determined; a small decrease in R_h was observed with an increase in temperature.

9.2. PEO–PS block copolymers

Evidence for the formation of micelles in aqueous solutions of poly(styrene)–poly(ethylene oxide) (PS–PEO) block copolymers has been reported by Bahadur and Sastry [152], and Riess and Rogez [153]. The polymers were synthesized with ethylene oxide as the major component in order to make the copolymers water soluble, the polystyrene being extremely hydrophobic. The apparent molecular weight of PS–PEO micelles was found by Riess and Rogez [153] and Xu and co-workers [72,154] to increase with increasing copolymer molecular weight and decreasing PEO content. Diblock copolymers formed larger micelles than triblock copolymers. Bahadur and Sastry [152] found the micelle size to decrease with an increase in PS content, which shows that the micelle size also depends on the insoluble block. Increasing the temperature resulted in the formation of micelles with a smaller hydrodynamic radius. This is probably because water becomes a poorer solvent for ethylene oxide at higher temperatures, so the corona becomes less swollen with water, resulting in a decrease in the hydrodynamic radius; similar temperature effects have been observed in PEO–PPO–PEO copolymer micelles (see Section 5.1). Critical micellization concentrations of these PS–PEO block copolymers were estimated from the increase in the fluorescence intensity of pyrene with an increase in polymer concentration, and found to be in the order of 1–5 mg l^{-1} [155]. The micelle–water partition coefficient of pyrene was found to be in the order of 3×10^5, based on the polystyrene volume [155]. Gallot et al. [156] investigated micelle formation in methanol–water mixtures for several series of PEO–PS block copolymers, each having a constant PS chain length and varying lengths of the PEO block. Light scattering and small angle neutron scattering measurements carried out in methanol showed that the CMCs were primarily dependent on the molecular weight of the PS block and that, for a given molecular weight of the PS block, the aggregation number decreased with an increase in the PEO chain length. Despite the decrease in aggregation number, the hydrodynamic radius of the micelles was found to increase with PEO chain length. The SANS results showed the polystyrene core to be compact and small compared to the overall dimensions of the micelles, and the micelles to be spherical.

9.3. C_iE_j surfactants

It is interesting to compare the micellization of PEO–PPO–PEO block copolymers to that of C_iE_j (j-ethyleneglycol–i-alkyl ethers) low molecular-weight non-ionic surfactants [157,158], where both amphiphiles have a PEO headgroup. In the latter systems, it was found that the CMC

decreased and the micellar size increased strongly, both with increasing temperature. Thus, in these respects, the analogy between PEO–PPO copolymers and C_iE_j seems valid. However, the pronounced sensitivity of the CMC to temperature, or of the CMT to concentration observed for many PEO–PPO–PEO copolymers (see Sections 4.1, 5.1 and 5.2) is not evident with the *n*-alkyl poly(ethylene glycol) ethers, C_iE_j [159]. The decrease in hydrophilicity of the PEO blocks with increasing temperature has comparatively little effect on the CMC for C_iE_j [159]; in the case of PEO-PPO–PEO copolymer solutions, a 10 K decrease in temperature resulted in changes in the CMC of more than an order of magnitude [20,28]. The number of EO segments also has a small effect on the CMC of C_iE_j surfactants [157,159]; the change in CMC per EO segment for Pluronic copolymers was smaller than an equivalent change for the C_iE_j, indicating that the influence of the PEO block on CMC diminishes as the size of the surfactant increases. The main determinant of the CMC for C_iE_j was found to be the length of the alkyl (hydrophobic) chain. The logarithm of CMC for the C_iE_8, $i = 10$–15, series decreased linearly with increasing carbon number in the alkyl chain (CMC varied by approximately 2.5 orders of magnitude over the carbon number range studied) [158].

The free energy of micellization, ΔG°, decreased with increasing number of carbon atoms in the alkyl chain, and with increasing temperature for *j*-ethyleneglycol–*i*-alkyl ethers with the same headgroup (PEO) and varying hydrophobic tail [158,160]. Free energy changes for micelle formation per methylene group were equal to -0.69 kcal mol^{-1}, or -2.887 kJ mol^{-1}, to be compared with a ΔG°_{-PO-} of approximately -0.45 kJ mol^{-1} [30,69,76] for the PEO–PPO–PEO copolymers. ΔH° decreased with increasing carbon number, while $T\Delta S^\circ$ increased, indicating that ΔS° contributes mainly to micellization, while ΔH° counteracts micellization. The headgroup contribution to ΔG° decreased with increasing temperature, attributed to dehydration of the PEO chain. For *j*-ethyleneglycol–*i*-alkyl ethers with the same hydrophobic tail and varying PEO headgroup (e.g. for the system $C_{16}E_j$, $j = 17, 32, 44, 63$ [157]) ΔG° increased (became less negative) with increasing number of EO segments in the hydrophilic headgroup, and decreased with increasing temperature. ΔH° and ΔS° decreased with increasing number of EO segments, while the headgroup contribution to ΔG° increased with increasing number of EO segments.

10. Select applications of block copolymer solutions

10.1. Solubilization of organics

An interesting property of aqueous micellar systems is their ability to enhance the solubility in water of otherwise water-insoluble hydrophobic compounds. This occurs because the core of the micelle provides a hydrophobic microenvironment, suitable for solubilizing such molecules. The phenomenon of solubilization forms the basis for many practical applications of amphiphiles. The enhancement in the solubility of lyophobic solutes in solvents afforded by amphiphilic copolymer micelles has shown promise in many industrial and biomedical applications [17].

The solubilization of para-substituted acetanilides in a series of Pluronic PEO PPO–PEO triblock copolymers depended on both the copolymer composition and the nature of the solubilizate [161]. The more hydrophobic halogenated acetanilides exhibited a decrease in solubility with an increase in the copolymer PEO content, whereas the opposite trend was noted with less hydrophobic drugs such as acetanilide and the hydroxy-, methoxy-, and ethoxy-substituted compounds. The solubility of indomethacin in aqueous solutions of PEO–PPO–PEO copolymers was studied by Lin and Kawashima [7]. This hydrophobic anti-inflammatory drug was solubilized in significant amounts only above a certain threshold copolymer concentration, most likely related to the CMC. The solubilizing capacity increased with polymer molecular weight and solution temperature. Approximately 0.5 mol indomethacin per mol of copolymer could be solubilized in the copolymer solutions [7].

Nagarajan et al. [15] studied the solubilization of aromatic and aliphatic hydrocarbons in solu-

tions of PEO–PPO and poly(*N*-vinylpyrrolidone–styrene) (PVP–PS) copolymers. A 10 wt.% solutions of 12 500 molecular weight PEO–PPO (70:30) copolymer (of undefined blockiness), and a 20% solution of poly(*N*-vinylpyrrolidone–styrene) (40:60) were used. More hydrocarbon was solubilized per gramme of polymer in the PVP–PS copolymer than in the PEO–PPO copolymer, for both aromatic and aliphatic hydrocarbons. This is probably due to the fact that the PEO–PPO copolymer contained only 30% of the hydrophobic PPO constituent, whereas the PVP–PS copolymer contained 60% PS, and that the PS is more hydrophobic than PPO. It was also observed that aromatic hydrocarbons were solubilized in larger amounts than the aliphatic hydrocarbons [15]. A Flory–Huggins type interaction parameter between the solubilizate and the polymer block constituting the core, χ_{sc}, was estimated using Hildebrand–Scatchard solubility parameters. The aromatic hydrocarbons, which had smaller values of χ_{sc}, were found to solubilize to a greater extent than the aliphatic molecules, which had larger values of χ_{sc}. However, there was not a direct correlation between χ_{sc} and the amount solubilized, particularly for the aliphatic molecules which had large χ_{sc} values. For binary mixtures of benzene and hexane, it was shown that the micelles selectively solubilized the aromatic benzene.

An extensive study of the effect of copolymer structure on the solubilization of naphthalene in a range of PEO–PPO–PPO block copolymers has been reported by Hurter et al. [17]. Enhanced solubility of naphthalene in Pluronic copolymer solutions can be achieved; Fig. 26 shows the relationship between the micelle/water partition coefficient of naphthalene, K_{mw}, and the PPO content of the polymer ($K_{mw} = C^s_m/C^s_w$, and C^s_m, C^s_w are the concentrations of naphthalene in the micelle, based on total polymer mass, and in the water respectively). The solubility of naphthalene in the micellar solution is enhanced as the copolymer PPO/PEO composition ratio increases, at a certain total copolymer concentration. If K_{mw} is normalized with PPO content (denoted by K'_{mw}), there is still a small increase in the partition coefficient with increased PPO content in the polymer, which suggests that structural changes within the micelle, as a result of changes in polymer composition, must be influencing the partitioning behavior. For the majority of copolymers studied by Hurter et al. [17], the partition coefficient was found to be constant over the entire polymer concentration range probed. A linear relationship between the copolymer concentration and the amount of naphthalene solubilized (Fig. 26) is an indication that the micellar structure does not change significantly in this concentration range, and that increasing the polymer concentration leads to an increase in the number of micelles

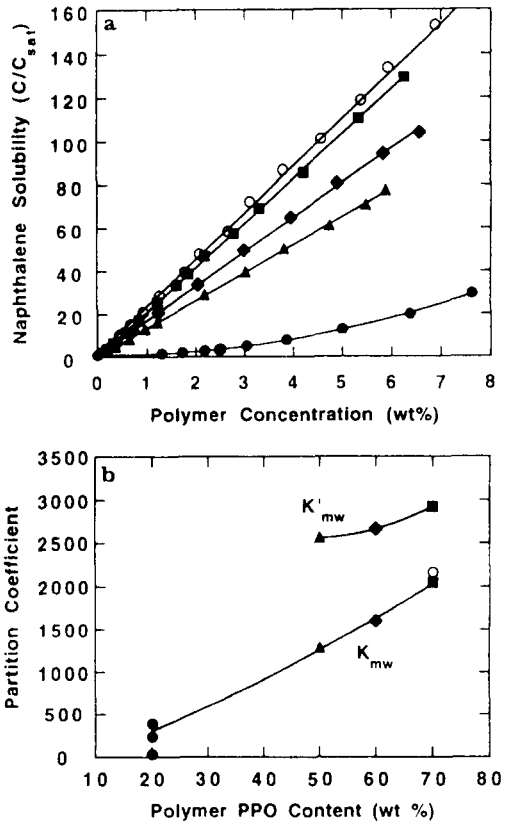

Fig. 26. (a) Solubility of naphthalene in Pluronic PEO–PPO–PEO copolymers: ○, P123; ■, P103; ◆, P104; ▲, P105; ●, F108. (b) Relationship between the micelle/water partition coefficient of naphthalene in Pluronic copolymer micelles, K_{mw}, and the PPO content of the polymer ($K_{mw} = C^s_n/C^s_w$, and C^s_m, C^s_w are the concentrations of naphthalene in the micelle, based on total polymer mass, and in the water respectively; K^1_{mw} is K_{mw} normalized with respect to the PPO content). (Reprinted with permission from Ref. [16]; copyright American Chemical Society, 1992.)

rather than micellar growth [17]. The solubilization of 1,6-diphenyl-1,3,5-hexatriene (DPH), a fluorescence dye, in Pluronic copolymer micellar solutions was investigated by Alexandridis and co-workers [76,162]. DPH partitioned favorably in the micellar phase, with a partition coefficient that was highest for P123 (a Pluronic copolymer with 70% PPO) and decreased in the order P123 > P103 > P104 = P105 > F127 > P84 > P85 = F108 > F88 > F68 > P65. It can be concluded from these data that the solubilization was influenced by both the relative (with respect to PEO) and absolute size of the hydrophobic PPO block.

10.2. Protection of microorganisms

Insect and mammalian cells are becoming important in the biotechnology industry for the production of complex proteins. These cells are sensitive to shear, and are thus difficult to grow to high cell concentrations such as those found in fermentation for the production of antibiotics. Cell death occurs during sparging because of high shear. PEO–PPO–PEO copolymers have been shown to protect mammalian cells from such damage.

Murhammer and Goochee [12,163] examined the structural features of non-ionic polyglycol copolymer molecules responsible for the protective effect in sparged animal cell bioreactors. It was shown that the same Pluronic copolymers that did not inhibit cell growth were the ones that provided protection from sparging in the bioreactors used in this study. The protective ability of Pluronics was found to correlate with the hydrophilic–lipophilic balance (HLB); the copolymers with the largest HLB (higher PEO content) were the protective agents. The PEO–PPO–PEO copolymers studied were more effective than homopolymer PEO in protecting the microorganisms. Supplementing the cell culture medium with 0.2% Pluronic L35 provided significantly more protection for cells growing in a Kontes airlift bioreactor than addition of 0.2% Pluronic F68 [12]. It was demonstrated, however, that increasing the F68 concentration to 0.5%, which results in a molar concentration comparable to that of 0.2% L35, provided significant cell protection; L35 and F68 appear thus to be comparable protective agents on a molar basis [163]. Zhang et al. [13] measured the mechanical properties of hybridoma cells taken from a continuous culture in the presence or absence of Pluronic F68 in the culture medium. The mean bursting membrane tension and the mean elastic area compressibility modulus of the cells were significantly greater in a medium containing 0.05% F68, compared to that without Pluronic copolymer. The short-term effect of Pluronic copolymer was also tested by its addition at various levels up to 0.2% immediately before the mechanical property measurements; a significant short-term effect could only be detected above a threshold copolymer concentration of 0.1% [13]. Orton [14] found Pluronic F68 to provide significant protection in mammalian cells in a sparged bubble column reactor. It was observed that, when F68 was present in the medium, cells no longer attached to bubbles and tended to aggregate less among themselves. A shedding effect was also visualized [14]: on a bubble formed in a medium without F68, the cells were found to be associated with the bubble surface, whereas cells were quickly shed from the gas–liquid interface in the presence of Pluronic F68.

10.3. Medical applications of PEO–PPO–PEO copolymers

"Microcontainers" for drug targeting using Pluronic PEO–PPO–PEO block copolymers were prepared by Kabanov and co-workers [10,164]. In order to target such microcontainers to a certain cell, the copolymer molecules were conjugated with antibodies against a target-specific antigen or with protein ligands selectively interacting with target cell receptors; proteins were attached to aldehyde group containing Pluronic molecules using the reductive alkylation reaction. The obtained conjugates were then incorporated into micelles containing solubilized drugs (such as fluorescein isothiocyanate (FITC) and haloperidol) by simple mixing of the corresponding components. It was found that solubilization of FITC in Pluronic copolymer micelles considerably influenced the distribution of FITC in animal (mouse) tissues, and resulted in a drastic increase of FITC fluorescence in the lung. The penetration efficiency of FITC in

lung tissues increased with increasing PEO–PPO–PEO copolymer hydrophobicity in the series F68, P85, L64. Such behavior was attributed to either different partitioning properties of Pluronic copolymers in tissue membranes or differences in micelle size. Conjugation of FITC-containing micelles with insulin vector resulted in increased FITC penetration in all tissues, including the brain. Specific targeting of the solubilized FITC in the brain was observed when a Pluronic conjugate with antibodies to the antigen of brain glial cell (a_2-glycoprotein) was incorporated into the micelles. A considerable increase of FITC fluorescence in the brain and decrease of its fluorescence in the lungs had been registered under these conditions. The possibility of using micellar microcontainers for targeting neuroleptics (haloperidol) in the brain was also studied. Incorporation of antibodies to a_2-glycoprotein into haloperidol-containing micelles resulted in a drastic increase of the effectiveness of the drug, indicating that vector-containing Pluronic copolymer micelles can effectively transport solubilized neuroleptics across the blood–brain barrier. The same research group also demonstrated that a low-molecular-weight compound (ATP), solubilized in Pluronic micelles, acquires the ability to penetrate within an intact cell in vitro [165].

Gels formed by Pluronic PEO–PPO–PEO copolymers were evaluated by Guzman et al. [9] as media for the subcutaneous administration of drugs; phenolsulfophthalein (PR) was used as a tracer. The type of Pluronic copolymer (F108 or F127), their concentrations, and the effect of solutes (NaOH, NaCl or PR) on gelation properties were studied; sodium hydroxide and sodium chloride decreased the gel–sol transition temperature, whereas the opposite effect was observed with PR. The in vitro release rates obtained for PR were inversely proportional to the concentration of copolymer used and a zero-order release rate was observed in all preparations assayed. The amount released at a given time was smaller at high polymer concentrations; this was attributed to the gel matrix being more rigid. Pluronic F127/PR preparations were administered subcutaneously to Wistar rats; PR plasma levels were compared with those reached after subcutaneous or intravenous administration of a PR aqueous solution. The gel formulation produced a sustained plateau level within 15 min that lasted 8–9 h. Good fits for experimental in vivo data from Pluronic gels were obtained using a zero-order input and first-order output two-compartment pharmacokinetics model; the fitted parameters of the model indicate that release of PR from the gel controlled the PR absorption process. The results obtained suggest that F127 aqueous gels may be of practical use as media for the subcutaneous administration of drugs.

The adsorption of PPO–PEO copolymers at surfaces as a means of preventing protein adsorption at these surfaces has been explored by Lee et al. [166] and Amiji and Park [167]. Proteins adsorb to almost all surfaces during the first few minutes of blood exposure. There has been much effort in minimizing or eliminating protein adsorption, as surfaces that exhibit minimal protein adsorption are important in many applications, including devices that come into contact with blood, membranes for separation processes, contact lenses, etc. [166]. Lee et al. [166] found the adsorption of human albumin on low density polyethylene (LDPE) surfaces treated with copolymer to be significantly less than on the untreated surface. The protein resistance to the copolymer-treated surface was highly dependent on the amount of copolymer adsorbed and on the mobility of the PEO segments. Star-like PEO–PPO block copolymers were found to have better adsorption properties than triblocks. Despite the favorable results, the authors voice concern over the stability of the adsorbed copolymer layer and the possible desorption of the copolymers into the treated medium [166]. Note also that, because of competitive adsorption between copolymers and proteins, and desorption of the copolymer blocks, ambiguities may be introduced in protein adsorption studies.

Adsorption of fibrinogen and platelet adhesion onto dimethyldichlorosilane-treated glass and LDPE surfaces treated with PEO homopolymer and various PEO–PPO–PEO block copolymers was examined by Amiji and Park [167]. PEO could not prevent platelet adhesion and activation, even when the bulk PEO concentration for adsorp-

tion was increased to 10 mg ml^{-1}. Pluronic copolymers containing 30 PO segments could not prevent platelet adhesion and activation, although the number of EO segments varied up to 76. Pluronics containing 56 PO segments inhibited platelet adhesion and activation, although the number of EO segments was as small as 19. Fibrinogen adsorption on the Pluronic-coated surfaces was reduced by more than 95% compared to adsorption on control surfaces. The ability of Pluronic copolymers to prevent platelet adhesion and activation was mainly dependent on the number of PO segments, rather than the number of EO segments [167]. This was contrary to the findings of Luo et al. [147] who suggested that copolymers with large PPO blocks do not adsorb well because they form micelles in solution; it should be noted, however, that the number of Pluronic copolymers studied by Luo et al. was rather limited. According to Amiji and Park [167], the PO segments were responsible for attaching the copolymer to the surface, and the EO segments for repelling fibrinogen and platelets by a steric repulsion mechanism.

11. Dynamics of micelle and gel formation

The kinetics of micelle formation in aqueous solutions of low-molecular-weight surfactants have attracted considerable attention. In general, two relaxation processes have been observed: a fast process (μs–ms time range) attributed to a surfactant molecule entering or exiting a micelle, and a slower process (ms–s time range) due to micelle assembly or dissociation [168]. The large molecular weight and chain-like structure of block copolymer molecules are expected to complicate the processes of micelle formation and exchange of copolymer molecules between micelles and the bulk solution; disentanglement of copolymer molecules from the micelles should result in time-scales slower than those observed in conventional surfactants. Linse and Malmsten [25] and Malmsten and Lindman [59] followed the temperature dependence of the Pluronic F127 micellization process by performing gel-permeation chromatography (GPC) experiments at different temperatures. The micelle fraction appeared as a separate peak in the chromatogram; this led the authors to the conclusion that the residence time of the polymer molecules in the F127 PEO–PPO–PEO micelles is extremely long (hours). However, Fleischer [65] reported that the lifetime of a copolymer molecule within the micelle was shorter than the minimum observation time of the experiments ($\approx$3 ms). He reached this conclusion from PFG-NMR measurements of F127 copolymer self-diffusion. Since unimers and micelles coexist in the solution, Fleischer expected to observe two self-diffusion coefficients, one for the unimers and one for the micelles, if there were no exchange of the molecules between the two states within the diffusion time. A single diffusion coefficient was, nevertheless, observed, and thus Fleischer [65] inferred that the copolymer solution was in the dynamic range of fast exchange.

The kinetics of gelation for aqueous solutions of Pluronic F98 and F127 PEO–PPO–PEO copolymers were investigated by Wang and Johnston [138] with the help of pulse shearometry. The pulse shearometer was designed to measure the propagation velocity (and from this the dynamic shear modulus) of a shear wave through a viscoelastic material that has been subjected to conditions of non-steady shear. Three distinct linear phases were observed for the log (dynamic shear modulus, G') vs. time profiles, as copolymer solutions of varying concentrations were allowed to passively warm at room temperature to a temperature exceeding the sol-to-gel transition temperature, T_m. The initial exponential phase was due to warming, while the beginning of the second exponential phase coincided with the onset of the gelation process as determined by visual observation. The third exponential phase was attributed to the rate of formation of the polymer network (gelation appeared to be complete at the beginning of this phase). A comparison of F127 (30%, T_m = 10.9 C) and F98 (37%, T_m = 11.1 C) would suggest that the concentration of copolymer required to achieve a certain gelation temperature decreases with increasing molecular weight of the PPO block of the copolymer. Characteristic times for gelation were 17 and 9 min for 20 and 30% F127, respectively, and 43 and 30 min for 20 and 30% F98, respectively. The gelation process was more rapid

for F127 (at a given concentration) and the characteristic times decreased with increasing concentration for a given copolymer. Wang and Johnston [138] suggested that the rate of gelation for the Pluronic solutions studied was dependent on the rate of heat transfer through the polymer solution (copolymer solutions were allowed to passively warm at room temperature). If this statement is true then the attribution by the authors of the time-dependent results to "kinetics of gelation" is erroneous, and the time-scales they reported were actually kinetics of heat transfer. It becomes obvious from the above that the dynamics of block copolymer micelle and gel formation, although important from both a theoretical and a practical point of view, are still unexplored and not well understood.

12. Conclusions

The phase behavior and aggregation properties of poly(ethylene oxide)–*block*–poly(propylene oxide)–*block*-poly(ethylene oxide) (PEO–PPO–PEO) copolymers in solution, as affected by the copolymer molecular composition and concentration, additives, and solution temperature, are important in understanding the mechanism of copolymer action underlying the various applications. While the PEO–PPO–PEO copolymers exist in solution as individual coils (unimers) at low temperatures and/or concentrations, micelles are formed on increasing the copolymer concentration and/or solution temperature, as revealed by surface tension, light scattering, and dye solubilization experiments. The unimer-to-micelle transition is not sharp, but spans a concentration decade or 10 K. The critical micellization concentration (CMC) and temperature (CMT) decrease with increase in the copolymer PPO content or molecular weight, and in the presence of salts. The dependence of CMC on temperature together with differential scanning calorimetry measurements indicate that the micellization process of PEO–PPO–PEO copolymers in water is endothermic, and is driven by the entropy gain in water when unimers aggregate to form micelles (hydrophobic effect) and the decrease in polarity of EO and PO as temperature increases. The free energy and enthalpy of micellization can be correlated to the number of EO and PO segments in the copolymer and the copolymer molecular weight. The PEO–PPO–PEO copolymers form micelles with hydrodynamic radii of approximately 10 nm and aggregation numbers in the order of 50. The aggregation number is thought to be independent of concentration and to increase with temperature. Despite the latter, the micelle hydrodynamic radii are generally independent of temperature, a result of dehydration of the PEO segments at elevated temperatures. Fluorescence molecules have been used to probe the microenvironment in block copolymer micelles. Phenomenological and mean-field lattice models for the formation of micelles can capture qualitatively the trends observed experimentally. A self-consistent mean-field theory was able to reproduce the anomalous phase behavior of PEO and PPO homopolymers, predict the micellization behavior of PEO–PPO–PEO block copolymers, and provide detailed information on the distribution of the copolymer segments in the micelles. The model calculations showed qualitative agreement with experimental predictions on the effect of temperature, concentration, hydrophobicity, and molecular weight of the polymer; quantitative agreement was also good, considering that all the model input parameters were obtained from independent experiments. The PEO–PPO–PEO copolymers adsorb on air–water and solid–water interfaces; for copolymers adsorbed at hydrophobic interfaces, the PPO block is located at the interface while the PEO block extends into the solution. Gels are formed by certain PEO–PPO–PEO block copolymers at high concentrations, while the micelles remain apparently intact in the form of a "crystal". The gelation onset temperature and the thermal stability range of the gel increase with increasing PEO block length.

References

[1] I.R. Schmolka, J. Am. Oil Chem. Soc., 54 (1977) 110.
[2] P. Bahadur and G. Riess, Tenside Surf. Det., 28 (1991) 173.

[3] I.R. Schmolka, Cosmetics and Toiletries, 95 (April 1980) 77.
[4] I.R. Schmolka, Cosmetics and Toiletries, 99 (November 1984) 69.
[5] F.M. Winnik, M.P. Breton and W. Riske, U.S. Patent 5,139,574, 1992.
[6] F.M. Winnik, A.R. Davidson, J.W.-P. Lin and M.D. Croucher, U.S. Patent 5,145,518, 1992.
[7] S.-Y. Lin and Y. Kawashima, Pharm. Acta Helv., 60 (1985) 339.
[8] M. Yokoyama, Crit. Rev. Therapeutic Drug Carrier Syst., 9 (1992) 213.
[9] M. Guzman, F.F. Garcia, J. Molpeceres and M.R. Aberturas, Int. J. Pharm., 80 (1992) 119.
[10] A.V. Kabanov, E.V. Batrakova, N.S. Melik-Nubarov, N.A. Fedoseev, T.Yu. Dorodnich, V.Yu. Alakhov, V.P. Chekhonin, I.R. Nazalova and V.A. Kabanov, J. Controlled Release, 22 (1992) 141.
[11] R.L. Henry and I.R. Schmolka, Crit. Rev. Biocompatibility, 5 (1989) 207.
[12] D.W. Murhammer and C.F. Goochee, Biotechnol. Prog., 6 (1990) 142.
[13] Z. Zhang, M. Al-Rubeai and C.R. Thomas, Enzyme Microbiol. Technol., 14 (1992) 980.
[14] D.E. Orton, Quantitative and Mechanistic Effects of Bubble Aeration on Animal Cells in Culture, Ph.D. Thesis, Massachusetts Institute of Technology, Cambridge, MA, 1992.
[15] R. Nagarajan, M. Barry and E. Ruckenstein, Langmuir, 2 (1986) 210.
[16] P.N. Hurter and T.A. Hatton, Langmuir, 8 (1992) 1291.
[17] P.N. Hurter, P. Alexandridis and T.A. Hatton, in S.D. Christian and J.F. Scamehorn (Eds.), Solubilization in Surfactant Aggregates, Marcel Dekker, New York, 1995, in press.
[18] Pluronic and Tetronic Surfactants, Technical Brochure, BASF Corp., Parsippany, NJ, 1989.
[19] R.J. Hunter, Foundations of Colloid Science, Vol. 1., Oxford University Press, New York, 1987.
[20] E.D. Goddard, C.A.J. Hoeve and G.C. Benson, J. Phys. Chem., 61 (1957) 593.
[21] Z. Zhou and B. Chu, J. Colloid Interface Sci., 126 (1988) 171.
[22] P. Mukerjee and K.J. Mysels, Critical Micelle Concentrations of Aqueous Surfactant Systems, NSRDS-NBS 36, Government Printing Office, Washington, DC, 1971.
[23] A. Sikora and Z. Tuzar, Makromol. Chem., 184 (1983) 2049.
[24] C. Price, Pure Appl. Chem., 55 (1983) 1563.
[25] P. Linse and M. Malmsten, Macromolecules, 25 (1992) 5434.
[26] N.K. Reddy, P.J. Fordham, D. Attwood and C. Booth, J. Chem. Soc., Faraday Trans., 86 (1991) 1569.
[27] W. Brown, K. Schillen, M. Almgren, S. Hvidt and P. Bahadur, J. Phys. Chem., 95 (1991) 1850.
[28] P. Alexandridis, J.F. Holzwarth and T.A. Hatton, Macromolecules, 27 (1994) 2414.
[29] A.A. Al-Saden, T.L. Whateley and A.T. Florence, J. Colloid Interface Sci., 90 (1982) 303.
[30] G. Wanka, H. Hoffmann and W. Ulbricht, Colloid Polym. Sci., 266 (1990) 101.
[31] F. Grieser and C.J. Drummond, J. Phys. Chem., 92 (1988) 5580.
[32] N.J. Turro and C. Chung, Macromolecules, 17 (1984) 2123.
[33] A. Chattopadhyay and E. London, Anal. Biochem., 139 (1984) 408.
[34] K.P. Ananthapadmanabhan, E.D. Goddard, N.J. Turro and P.L. Kuo, Langmuir, 1 (1985) 352.
[35] D.A. Edwards, R.G. Luthy and Z. Liu, Environ. Sci. Technol., 25 (1991) 127.
[36] I.R. Schmolka and A.J. Raymond, J. Am. Oil Chem. Soc., 42 (1965) 1088.
[37] P. Alexandridis, T. Nivaggioli and T.A. Hatton, Langmuir, in press.
P. Alexandridis, T. Nivaggioli, J.F. Holzwarth and T.A. Hatton, Polym. Prepr. (Am. Chem. Soc., Div. Polym. Chem.), 35(1) (1994) 604.
[38] Z. Tuzar and P. Kratochvil, Adv. Colloid Interface Sci., 6 (1976) 201.
[39] D. Attwood and A.T. Florence, Surfactant Systems: Their Chemistry, Pharmacy and Biology, Chapman and Hall, London, 1983.
[40] G.-E. Yu, Y. Deng, S. Dalton, Q.-G. Wang, D. Attwood, C. Price and C. Booth, J. Chem. Soc., Faraday Trans., 88 (1992) 2537.
[41] P.C. Hiemenz, Principles of Colloid and Surface Chemistry, 2nd edn., Marcel Dekker, New York, 1986, p 446.
[42] C. Tanford, The Hydrophobic Effect: Formation of Micelles and Biological Membranes, 2nd edn., Wiley, New York, 1980.
[43] A. Ben-Naim, Hydrophobic Interactions, Plenum, New York, 1980.
[44] R. Kjelander and E. Florin, J. Chem. Soc., Faraday Trans. 1, 77 (1981) 2053.
[45] R.E. Goldstein, J. Chem. Phys., 80 (1984) 5340.
[46] G. Karlstrom, J. Phys. Chem., 89 (1985) 4962.
[47] B. Lindman, A. Carlsson, G. Karlstrom and M. Malmsten, Adv. Colloid Interface Sci., 32 (1990) 183.
[48] P.N. Hurter, J.M.H.M. Scheutjens and T.A. Hatton, Macromolecules, 26 (1993) 5030.
[49] P.N. Hurter, J.M.H.M. Scheutjens and T.A. Hatton, Macromolecules, 26 (1993) 5592.
[50] P. Linse, Macromolecules, 26 (1993) 4437.
[51] P. Linse, J. Phys. Chem., 97 (1993) 13896.
[52] J.K. Armstrong, J. Parsonage, B. Chowdhry, S. Leharne, J. Mitchell, A. Beezer, K. Lohner and P. Laggner, J. Phys. Chem., 97 (1993) 3904.
[53] A. Beezer, N. Mitchard, J.C. Mitchell, J.K. Armstrong, B. Chowdhry, S. Leharne and G. Buckton, J. Chem. Res. (S), (1992) 236.

[54] N.M. Mitchard, A.E. Beezer, J.C. Mitchell, J.K. Armstrong, B.Z. Chowdhry, S. Leharne and G. Buckton, J. Phys. Chem., 96 (1992) 9507.
[55] R.K. Williams, M.A. Simard and C. Jolicoeur, J. Phys. Chem., 89 (1985) 178.
[56] Z. Zhou and B. Chu, Macromolecules, 21 (1987) 2548.
[57] W. Brown, K. Schillen and S. Hvidt, J. Phys. Chem., 96 (1992) 6038.
[58] M. Almgren, P. Bahadur, M. Jansson, P. Li, W. Brown and A. Bahadur, J. Colloid Interface Sci., 151 (1992) 157.
[59] M. Malmsten and B. Lindman, Macromolecules, 25 (1992) 5440.
[60] M. Malmsten and B. Lindman, Macromolecules, 25 (1992) 5446.
[61] K. Mortensen, Europhys. Lett., 19 (1992) 599.
[62] K. Mortensen, W. Brown and B. Norden, Phys. Rev. Lett., 68 (1992) 3240.
[63] K. Mortensen and W. Brown, Macromolecules, 26 (1993) 4128.
[64] K. Mortensen and J.S. Pedersen, Macromolecules, 26 (1993) 805.
[65] G. Fleischer, J. Phys. Chem., 97 (1993) 517.
[66] G. Fleischer, P. Bloss and W.D. Hergerth, Colloid Polym. Sci., 271 (1993) 217.
[67] K. Pandya, P. Bahadur, T.N. Nagar and A. Bahadur, Colloids and Surfaces, 70 (1993) 219.
[68] K. Pandya, P. Bahadur and A. Bahadur, Tenside Surf. Det., 31 (1994) 182.
[69] G. Wanka, H. Hoffmann and W. Ulbricht, Macromolecules, 27 (1994) 4145.
[70] T. Nivaggioli, P. Alexandridis, T.A. Hatton, A. Yekta and M.A. Winnik, Langmuir, in press.
[71] A. Halperin, Macromolecules, 20 (1987) 2943.
[72] R. Xu, M.A. Winnik, G. Riess, B. Chu and M.D. Croucher, Macromolecules, 25 (1992) 644.
[73] D. Attwood, J.H. Collet and C.J. Tait, Int. J. Pharm., 26 (1985) 25.
[74] J.C. Gilbert, C. Washington, M.C. Davies and J. Hadgraft, Int. J. Pharm., 40 (1987) 93.
[75] M. Almgren, J. Alsins and P. Bahadur, Langmuir, 7 (1991) 446.
[76] P. Alexandridis, Thermodynamics and Dynamics of Micellization and Micelle–Solute Interactions in Block-Copolymer and Reverse Micellar Systems, Ph.D. Thesis, Massachusetts Institute of Technology, Cambridge, MA, 1994.
[77] J.K. Thomas, The Chemistry of Excitation at Interfaces, ACS Monograph 181, Washington, DC, 1984, Chapter 5.
R. Zana (Ed.), Surfactant Solutions: New Methods of Investigation, Marcel Dekker, New York, 1986.
M.A. Winnik, O. Pekcan and M.D. Croucher, in F. Candau and R.H. Ottewill (Eds.), Scientific Methods for the Study of Polymer Colloids and their Applications, Kluwer, Amsterdam, 1990, pp. 225–245.
[78] D. Georgescauld, J.P. Desmasez, R. Lapouyade, A. Babeau, H. Richard and M. Winnik, Photochem. Photobiol., 31 (1980) 539.
F.M. Winnik, M.A. Winnik, H. Ringsdorf and J. Venzmer, J. Phys. Chem., 95 (1991) 2583.
A. Yekta, J. Duhamel, P. Brochard, H. Adiwidjaja and M.A. Winnik, Macromolecules, 26 (1993) 1829.
[79] T. Nivaggioli, P. Alexandridis and T.A. Hatton, INFORM, 5(4) (1994) 524.
T. Nivaggioli, P. Alexandridis, B. Tsao and T.A. Hatton, Langmuir, in press.
[80] K. Nakashima, T. Anzai and Y. Fujimoto, Langmuir, 10 (1994) 658.
[81] T. Landh, J. Phys. Chem., 98 (1994) 8453.
[82] P. Bahadur, K. Pandya, M. Almgren, P. Li and P. Stilbs, Colloid Polym. Sci., 271 (1993) 657.
[83] P. Bahadur, P. Li, M. Almgren and W. Brown, Langmuir, 8 (1992) 1903.
[84] M.H.G.M. Penders, S. Nilsson, L. Piculell and B. Lindman, J. Phys. Chem. 98 (1994) 5508.
[85] P. Alexandridis, V. Athanassiou and T.A. Hatton, Langmuir, submitted for publication.
[86] M. Almgren, J.v. Stam, C. Lindblad, P. Li, P. Stilbs and P. Bahadur, J. Phys. Chem., 95 (1991) 5677.
[87] E. Hecht and H. Hoffmann, Langmuir, 10 (1994) 86.
[88] L. Leibler, H. Orland and J.C. Wheeler, J. Chem. Phys., 79 (1983) 3550.
[89] J. Noolandi and K.M. Hong, Macromolecules, 16 (1983) 1443.
[90] M.R. Munch and A.P. Gast, Macromolecules, 21 (1988) 1360.
[91] R. Nagarajan and K. Ganesh, J. Chem. Phys., 90 (1989) 5843.
[92] C.M. Marques, Macromolecules, 21 (1988) 1051.
[93] A.N. Semenov, Sov. Phys. JETP, 61 (1985) 733.
[94] Y.B. Zhulina and T.M. Birshtein, Polym. Sci. USSR (Engl. Transl.), 12 (1986) 2880.
[95] B. van Lent and J.M.H.M. Scheutjens, Macromolecules, 22 (1989) 1931.
[96] Y. Wang, W.L. Mattice and D.H. Napper, Langmuir, 9 (1993) 66.
[97] O. Prochazka, Z. Tuzar and P. Kratochvil, Polymer, 32 (1991) 3038.
[98] P. Flory, Principles of Polymer Chemistry, Cornell University, Ithaca, NY, 1953.
[99] D. Izzo and C.M. Marques, Macromolecules, 26 (1993) 7189.
[100] G. ten Brinke and G. Hadziioannou, Macromolecules, 20 (1987) 486.
[101] N.P. Balsara, M. Tirrell and T.P. Lodge, Macromolecules, 24 (1991) 1975.
[102] J.M.H.M. Scheutjens and G.J. Fleer, J. Phys. Chem., 83 (1979) 1619.
[103] F.A.M. Leermakers, P.P.A.M. van der Schoot, J.M.H.M. Scheutjens and J. Lyklema, in K.L. Mittal (Ed.), The Equilibrium Structure of Micelles, Plenum, New York, 1989.
[104] F.A.M. Leermakers and J.M.H.M. Scheutjens, J. Phys. Chem., 93 (1989) 7417.
[105] D.G. Hall and B.A. Pethica, in M.J. Schick (Ed.),

Nonionic Surfactants, Marcel Dekker, New York, 1967, Chapter 16.
[106] T.L. Hill, Thermodynamics of Small Systems, Vol. 1, Benjamin, 1963.
[107] T.L. Hill, Thermodynamics of Small Systems, Vol. 2, Benjamin, 1964.
[108] O.A. Evers, J.M.H.M. Scheutjens and G.J. Fleer, Macromolecules, 23 (1990) 5221.
[109] J.M.H.M. Scheutjens and G.J. Fleer, Macromolecules, 18 (1985) 1882.
[110] J.M.H.M. Scheutjens, F.A.M. Leermakers, N.A.M. Besseling and J. Lyklema, in K.L. Mittal, (Ed.), Surfactants in Solution, Vol. 7, Plenum, New York, 1989.
[111] F.A.M. Leermakers, Ph.D. Thesis, Wagenigen Agricultural University, Wagenigen, 1988.
[112] P. Alexandridis, V. Athanassiou, S. Fukuda and T.A. Hatton, Langmuir, 10 (1994) 2604.
[113] D.K. Chattoraj and K.S. Birdi, Adsorption and the Gibbs Surface Excess, Plenum, New York, 1984.
[114] K.N. Prasad, T.T. Luong, A.T. Florence, J. Paris, C. Vaution, M. Seiller and F. Puisieux, J. Colloid Interface Sci., 69 (1979) 225.
[115] R.A. Anderson, Pharm. Acta Helv., 47 (1972) 304.
[116] P. Bahadur and K. Pandya, Langmuir, 8 (1992) 2666.
[117] K.J. Mysels, Langmuir, 2 (1986) 423.
[118] E.H. Crook, D.B. Fordyce and G.F. Trebbi, J. Phys. Chem., 67 (1963) 1987.
[119] A.F. Gallaugher and H. Hibbert, J. Am. Chem. Soc., 59 (1937) 2514.
[120] P. Lo Nostro and G. Gabrielli, Langmuir, 9 (1993) 3132.
[121] J.S. Phipps, R.M. Richardson, T. Cosgrove and A. Eaglesham, Langmuir, 9 (1993) 3530.
[122] A.R. Rennie, R.J. Crawford, E.M. Lee, R.K. Thomas, T.L. Crowley, S. Roberts, M.S. Qureshi and R.W. Richards, Macromolecules, 22 (1989) 3466.
[123] J.E. Glass, J. Phys. Chem., 72 (1969) 4459.
[124] M.J. Schwuger, J. Colloid Interface Sci., 43 (1973) 491.
[125] Y.J. Nikas, S. Puvvada and D. Blankschtein, Langmuir, 8 (1992) 2680.
[126] B. Kronberg, P. Stenius and Y. Thorssell, Colloids and Surfaces, 12 (1984) 113.
[127] M.S. Aston, T.M. Herrington and T.F. Tadros, Colloids and Surfaces, 51 (1990) 115.
[128] N.S. Santos Magalhaes, S. Benita and A. Baszkin, Colloids and Surfaces, 52 (1991) 195.
[129] S.G. Yeates, J.R. Craven, R.H. Mobbs and C. Booth, J. Chem. Soc., Faraday Trans. 1, 82 (1986) 1865.
[130] J.B. Kayes and D.A. Rawlins, Colloid Polym. Sci., 257 (1979) 622.
[131] H.R. Heydegger and H.N. Duning, J. Phys. Chem., 63 (1959) 1613.
[132] J.A. Baker and J.C. Berg, Langmuir, 4 (1988) 1055.
[133] J.A. Baker, R.A. Pearson and J.C. Berg, Langmuir, 5 (1989) 339.
[134] J. Lee, P.A. Martic and J.S. Tan, J. Colloid Interface Sci., 131 (1989) 252.
[135] E. Killmann, H. Maier and J.A. Baker, Colloids and Surfaces, 31 (1988) 51.
[136] F. Tiberg, M. Malmsten, P. Linse and B. Lindman, Langmuir, 7 (1991) 2723.
[137] M. Malmsten, P. Linse and T. Cosgrove, Macromolecules, 25 (1992) 2474.
[138] P. Wang and T.P. Johnston, J. Appl. Polym. Sci., 43 (1991) 283.
[139] I.R. Schmolka, J. Am. Oil Chem. Soc., 69 (1991) 206.
[140] J. Rassing and D. Attwood, Int. J. Pharm., 13 (1983) 47.
[141] M. Vadnere, G.L. Amidon, S. Lindenbaum and J.L. Haslam, Int. J. Pharm., 22 (1984) 207.
[142] J. Rassing, W.P. McKenna, S. Bandyopadhyay and E. Eyring, J. Mol. Liq., 27 (1984) 165.
[143] J.C. Gilbert, J.L. Richardson, M.C. Davies, K.J. Palin and J. Hadgraft, J. Controlled Release, 5 (1987) 113.
[144] M. Malmsten and B. Lindman, Macromolecules, 26 (1993) 1282.
[145] Y.-Z. Luo, C.V. Nicholas, D. Attwood, J.H. Collet, C. Price and C. Booth, Colloid Polym. Sci., 270 (1992) 1094.
[146] C.V. Nicholas, Y.-Z. Luo, N.-J. Deng, D. Attwood, J.H. Collet, C. Price and C. Booth, Polymer, 34 (1993) 138.
[147] Y.-Z. Luo, C.V. Nicholas, D. Attwood, J.H. Collet, C. Price, C. Booth, B. Chu and Z.-K. Zhou, J. Chem. Soc., Faraday Trans., 89 (1993) 539.
[148] W.-B. Sun, J.-F. Ding, R.H. Mobbs, F. Heatley, D. Attwood and C. Booth, Colloids and Surfaces, 54 (1991) 103.
[149] A.D. Beddels, R.M. Arafeh, Z. Yang, D. Attwood, F. Heatley, J.C. Padget, C. Price and C. Booth, J. Chem. Soc., Faraday Trans., 89 (1993) 1235.
[150] S. Tanodekaew, N.-J. Deng, S. Smith, Y.-W. Yang, D. Attwood and C. Booth, J. Phys. Chem., 97 (1993) 11847.
[151] A.J. Moment, P. Alexandridis and T.A. Hatton, in preparation.
[152] P. Bahadur and N.V. Sastry, Eur. Polym. J., 24 (1987) 285.
[153] G. Riess and D. Rogez, Polym. Prepr., (Am. Chem. Soc., Div. Polym. Chem.), 23 (1982) 19.
[154] R. Xu, M.A. Winnik, F.R. Hallett, G. Riess and M.D. Croucher, Macromolecules, 24 (1991) 87.
[155] M. Wilhelm, C.-L. Zhao, Y. Wang, R. Xu, M.A. Winnik, J.-L. Mura, G. Riess and M.D. Croucher, Macromolecules, 24 (1991) 1033.
[156] Y. Gallot, J. Selb, P. Marie and A. Rameau, Polym. Prepr. (Am. Chem. Soc., Div. Polym. Chem.), 23 (1982) 16.
[157] B.W. Barry and D.I.D. El-Eini, J. Colloid Interface Sci., 54 (1976) 339.
[158] K. Meguro, Y. Takasawa, N. Kawahashi, Y. Tabata and M. Ueno, J. Colloid Interface Sci., 83 (1981) 50.
[159] K. Meguro, M. Ueno and K. Esumi, in M.J. Schick (Ed.), Nonionic Surfactants: Physical Chemistry, Marcel Dekker, New York, 1987, p. 109.

[160] N. Nandi and I.N. Basumallick, J. Phys. Chem., 97 (1993) 3900.
[161] J.H. Colett and E.A. Tobin, J. Pharm. Pharmacol., 31 (1979) 174.
[162] P. Alexandridis, J.F. Holzwarth and T.A. Hatton, in preparation.
[163] D.W. Murhammer and C.F. Goochee, Biotechnol. Prog., 6 (1990) 391.
[164] A.V. Kabanov, V.I. Slepnev, L.E. Kuznetsova, E.V. Batrakova, V.Yu. Alakhov, N.S. Melik-Nubarov, P.G. Sveshnikov and V.A. Kabanov, Biochem. Int., 26 (1992) 1035.
[165] V.I. Slepnev, L.E. Kuznetsova, A.N. Gubin, E.V. Batrakova, V.Yu. Alakhov and A.V. Kabanov, Biochem. Int., 26 (1992) 587.
[166] J.-H. Lee, J. Kopecek and J.D. Andrade, J. Biomed. Mater. Res., 23 (1989) 351.
[167] M. Amiji and K. Park, Biomaterials, 13 (1992) 682.
[168] E.A.G. Aniansson, S.N. Wall, M. Almgren, H. Hoffmann, W. Ulbricht, R. Zana, J. Lang and C. Tondre, J. Phys. Chem., 80 (1976) 905.